MODELING BACTERIA-PRODUCE INTERACTION DURING WASHING: EFFECT OF SHEAR STRESS

By

YUYANG TIAN

A thesis submitted to the

School of Graduate Studies

Rutgers, The State University of New Jersey

In partial fulfillment of the requirements

For the degree of

Master of Science

Graduate Program in Food Science

Written under the direction of

Professor Mukund V. Karwe

And approved by

_____

_____

_____

New Brunswick, New Jersey

May 2018

ABSTRACT OF THE THESIS

MODELING BACTERIA-PRODUCE INTERACTION DURING WASHING: EFFECT OF SHEAR STRESS

by YUYANG TIAN

Thesis Director:

Professor Mukund V. Karwe

Due to increase in health awareness, there is an increase in the demand for fresh produce. The consumption of fresh produce has increased over the last few years. Most of the fresh produce is consumed raw or without any major processing steps before consumption. According to CDC report (2015 CDC annual report), more than 26% of the reported illnesses were associated with fresh produce. Safety of fresh produce is recognized as one of the significant challenges by the US Food and Drug Administration (FDA, 2015). Maintaining freshness, safety, and high-quality of fresh produce is essential for the industry to meet consumer demand.

Physical and chemical methods are commonly used for bacterial removal and inactivation during produce washing. While chemical methods are widely studied, a few studies show that shear stress has a significant effect on bacterial removal during produce washing. In this study, a numerical approach was used to understand the effect of shear stress on the attachment of bacteria to produce surface and the detachment of bacteria from a fresh produce surface.

COMSOL® Multiphysics was used to simulate turbulent flow in an experimental benchtop washing device to understand the effect of shear stress on (a) the detachment of bacteria from produce surface to wash water and (b) the attachment of bacteria to produce surface from wash water containing contaminated organic load. A 2D axisymmetric k-ε turbulent flow model with swirl flow was used in the numerical simulation. The geometry consisted of a downward facing rotating disk with a produce leaf attached at the center of the disk, in a tank filled with water. Single phase flow and a two-phase flow were simulated for detachment and attachment studies, respectively. The flow profiles and velocity vectors of the turbulent flow were obtained using numerical simulation. Shear stress distribution along the radius of the leaf was calculated numerically.

The results showed that the average shear stress exerted on the leaf surface was 28.3 mPa and 109 mPa, at 100 rev/min and 200 rev/min, respectively. Experimental results (from UC Davis) showed that the corresponding detachment of bacteria was about 1 log CFU/cm^2 and 1.5 log CFU/cm^2, respectively. In the attachment studies involving a two-phase flow of wash water and simulated organic particles, numerically predicted average shear stress values were 137 mPa and 403 mPa, at 100 rev/min and 200 rev/min, respectively. Predicted shear stress values were higher due to the suspended particles (beads). Experimental data showed that some (up to 0.4%) bacteria from the beads got transferred to the leaf surface suggesting that attachment can take place in the presence of shear stress.

The point-attachment model using ordinary differential equations to describe the ligand-receptor binding of bacteria and produce surface was used to quantify the detachment and attachment of bacteria from produce surface as a function of time. In the

mathematical model that we developed, shear and sanitizer concentration were included. MATLAB® was used to numerically solve the differential equations to study of the effect of detachment rate constant and the presence of sanitizers on the removal and transfer of bacteria. The detachment rate constant is effective in mediating the detachment and attachment of bacteria, in the absence of sanitizers in water. Nevertheless, the effect of detachment rate constant is shown not to be significant in the presence of a sanitizer during washing of produce.

Understanding the effect of shear stress on microbe - produce interaction will help improve the design of wash water systems and minimize the probability of cross contamination during washing process for fresh produce.

ACKNOWLEDGEMENTS

First and foremost, I would like to sincerely thank my advisor, Dr. Mukund V. Karwe, for his excellent guidance, encouragement and support throughout my Masters. I am really very grateful and honored to be provided the opportunity to participate in this project. This has been a great experience and wonderful academic training for me.

I would like to extend my sincere thanks to Dr. Deepti Salvi, for sharing her ideas, suggestions and for her great help and support throughout this whole project.

I would also like to thank my committee member, Dr. Matthews, for his critique of my thesis and his time.

I would like to thank Dr. Nitin Nitin and Dr. Kang Huang at UC Davis, for their tremendous help and support in the experiments, valuable experiences and suggestions given, and USDA NIFA under Federal Award No. 2015-68003-23411 sub-award No. 201403031-02 for providing the funding support for my research project. Progress reports and meetings throughout my masters years have been the record and witness of my academic growth. They are the treasures.

I would like to express my genuine thanks to my lovely lab mates, Karthik and Ender for all the technical support and mental guidance, and for creating a fun and lively research environment. Noopur, Isha, Shruthi, Yueming, Sawali for being such nice colleagues of working together, and for being lovely friends. Special thanks to Karthik, Ender and Noopur who I have come to consider as very close friends, for their support in and outside lab life during masters years.

I would also like to thank the staff at food science, Debbie, Irene, Laura, Rosanne, Madelaine, Yakov, Bill and Dave, for all of their help.

My sincere appreciation to my dear friends, especially Robyn and Jeff, for their encouragement and emotional support all the time. Thank you for being there for me.

Last but not least, no precise words of mine can adequately describe my thanks to my beloved parents, for their unconditional love and support and encouragement, and whose good examples have inspired me to work for harder. I am truly thankful to have you in life.

TABLE OF CONTENT

LIST OF FIGURES

LIST OF TABLES

1. INTRODUCTION

1.1. Research background: current status of food safety

In recent years, foodborne outbreaks related to fresh produce have become more and more of a concern. Safety of fresh produce is recognized as one of the significant challenges by the US Food and Drug Administration (FDA, 2015). Maintaining freshness, safety, and the quality of fresh produce is essential and has prompted more attention from the industry to reduce potential pathogen risks and enhance food safety, too meet the consumer demand.

Fresh-cut fruits and vegetables were considered as low risk produce in terms of food safety (Jensen et al., 2014). However, foodborne outbreaks in recent years have been more related to the less sanitary processing conditions of fresh-cut fruits and vegetables. The shelf life of fresh produce is often limited due to the presence of active spoilage microbes (Artés et al., 2009). According to CDC report (2009 CDC annual report), the outbreaks have shown that the water quality during post-harvest processing is critical for safety of fresh produce (Gil et al., 2009). The quality of water can be adversely affected by many factors including the organic load. The presence of organic matter in wash water decreases the efficacy of sanitizers, also increases the risk of cross-contamination since the organic matter enhances the transfer of bacteria. Since both of those two issues negatively impact the effectiveness of sanitizers and safety of fresh produce, there is a significant unmet need to evaluate the effect of organic matter on cross-contamination during postharvest washing and sanitizing of fresh produce.

1.2. Methods used to improve food safety

1.2.1. Physical treatments

Physical methods are effective in reducing the microorganisms from produce surface and usually employ the use of vigorous washing with water which generates shear force. Significant bacterial reduction has been achieved in lab scale experiments, using shear force, less so in industrialized processing (Gil et al., 2009). Other modern physical techniques to reduce the bacterial load in fresh produce processing include the use of ultrasound and high-pressure processing (HPP) (Gil et al., 2009). These physical techniques have shown efficacy in reducing the bacterial load from produce surface, and they are largely affected by the produce composition and are dependent on fresh produce types.

1.2.2. Chemical treatments

Chlorine sanitizer has been widely used for sanitation of fresh produce. Chlorine and chlorine-based derivatives have shown adequate disinfecting effects over fresh produce. Chlorine and chlorine-based derivatives have been used for over 30 years. However, the use of chlorine and its derivatives have been abused and have posed huge threat to the environment and also to human health for its excessive dosages (Gil et al., 2009). In the presence of organic matter in wash water, disinfecting agents such as chlorine can react with organic matter and further form harmful by-products such as trihalomethanes, haloacetic acids and chloropicrin (COT, 2007).

The maintenance of adequate wash water quality during washing has generated great attention and interest due to its importance in minimizing potential microbial

contamination of processing water, and subsequent cross contamination during processing of fresh produce (FDA, 2008). It was also found that wash water can mainly remove the microorganisms from fresh produce surface while the sanitizing agents can eliminate pathogens in the processing water. Water can also serve as a vehicle for cross contamination if not maintained at adequately safe level, especially during water reuse and recirculation (López-Gálvez et al., 2010). Research has shown that increasing the amount of water used in processing will not eliminate the risk of cross contamination. It was observed that cross-contamination can take place due to the presence of small amount of contaminated produce. Research has further confirmed the importance of combined use of water treatment and sanitizing agents. Sanitizers can inactivate microbes in wash water and minimize the possibility of further attachment and internalization of bacteria to fresh produce surface.

Combination of physical and chemical methods in removal and inactivation of microbes has shown promise in preventing cross-contamination during produce washing thus enhancing food safety. With proper coupling with physical treatment of water, effective doses of chemical sanitizing agents needed could be minimized.

1.3. Mechanisms of bacterial attachment

The adhesion of bacteria can be explained by classic and improved DLVO theory (Hermansson, 1999). DLVO theory is the short for Derjaguin-Landau-Verwey-Overbeek theory and it was initially proposed for qualitative colloidal stability study, and also to quantitatively calculate the adhesion free energy. In recent studies, researchers have discovered that the DLVO theory can be used for microbiological studies in terms of

bacterial adhesion. Qualitative models based on DLVO theory have been developed to predict adhesion behavior of microbes assuming that the behavior of microbial cells was similar to inert or chemical, non-biological particles.

The colonization of bacteria is common in nature and has been found on all inanimate biological surfaces. Once the adhesion of single bacterial cells occurs, the cells start to aggregate around it and a colonized group appears on the biological surface. The formation of biofilms as well as the adhesion of bacteria on biological surfaces play a significant role in commercial processing situations. The prevention of biofilm formation and the mechanism of bacterial adhesion have drawn great attention.

The classic DLVO theory divides the adhesion of bacteria into two phases. In the first phase, the bacteria behave as inert particles and they are manipulated by the physico-chemical interactions to attach to a surface. In the second phase where biofilms are likely to be formed, the aggregation of bacterial cells and the further proliferation occurs. The second phase of bacterial attachment can be seen as cell to cell interaction. Research has shown that the irreversible adhesion appears upon seconds of surface contact. In other words, the adhesion of bacteria to biological surfaces can be regarded as an instantaneous behavior. This transfer of bacteria via surface contact is irreversible and difficult to be removed spontaneously (Rijnaarts et al., 1995). Bacteria adhesion is generally regarded as the first step in biofilm formation. There are two mechanisms to describe microbial adhesion (Busscher et al., 2012):

a. Specific interactions between localized, specific molecular groups.
b. The bonding force of adhesion can be attractive Van der Waals forces, attractive or repulsive electrostatic, hydrogen bonding and Brownian motion forces.

It was suggested by Weiss et al. (1972) that the adhesion of bacteria is aided by reducing the contact area. The total adhesion free energy is reduced by reducing the radius of contact region, and by reducing the electrical interactions and van der Waals interactions between bacterial cells and biological surfaces. Atomic force microscopy has been used to measure the adhesion forces between bacteria and substratum surfaces directly. The adhesion to a surface is a survival mechanism of bacteria and nutrients in aqueous environment tend to accumulate at surfaces.

The irreversible adhesion was found by some researchers (Fletcher, 1988; Simoni et al., 1998) that the direct contact between bacterial cells and substratum surface is mediated and supported by surface polymers (Hermansson, 1999). Surface structures are believed to be involved in bacterial adhesion in that different cell surface structures contribute differently to the net cell charge and can further influence the potential adhesion of bacteria to surface. The roughness of contact surface was shown to affect the interaction energies. Bacteria reside in the grooves due to the roughness of surface are difficult to be washed off from substratum surfaces.

Single bacterial cells adhere very easily and attach to a substratum surface and the single cells tend to aggregate and (co)aggregate into large, complex microbial community termed as biofilms. By the definition of Bos et al. (1999), a biofilm is a layer of prokaryotic or eukaryotic cells anchoring to a substratum surface. In food industry, biofilm is regarded as a major threat to fresh produce safety and the prevention of which is of major concern of researchers and producers.

Bacteria adhesion to biomaterial surfaces has long been studied. It was suggested that both bacteria adhesion to substratum and the resistance of detachment from biological

surfaces are manipulated by specific and non-specific interactions (Vaudaux et al., 1990; Heilmann et al., 1996; Morra and Cassinelli, 1997; An and Friedman, 1998). These two interactions are dependent on the substratum properties and surrounding flow conditions.

Bacterial adhesion can be seen as a two-phase process which includes an instant, spontaneous and reversible physical phase as first phase, and an irreversible growing molecular and cellular second phase (An and Friedman, 1998). Take the example of the formation of *S. epidermidis* biofilm as shown in Fig. 1. The bacteria are initially attached to biomaterial surfaces. The attachment to the two different surfaces is via different mechanisms. The attachment to non-coated protein surface is mediated by physicochemical forces, i.e., hydrophobic interactions, electrostatic interactions, and van der Waals forces. The bacteria strains adhere and remain on the produce surface. Once the bacteria instantly attach on the surface, they start to aggregate and proliferate to form a monolayer of biomass of bacteria. The large clusters of bacteria are formed during the growth and proliferation process resulting in multilayer mixture of bacteria and extracellular material on the surface. The mature multilayer of biofilm is established by cell to cell interactions. The daughter bacterial cells which are loosely attached to the solid surface, detach from the polymer surface due to molecular and cellular, and physicochemical factors (Katsikogianni et al., 2004).

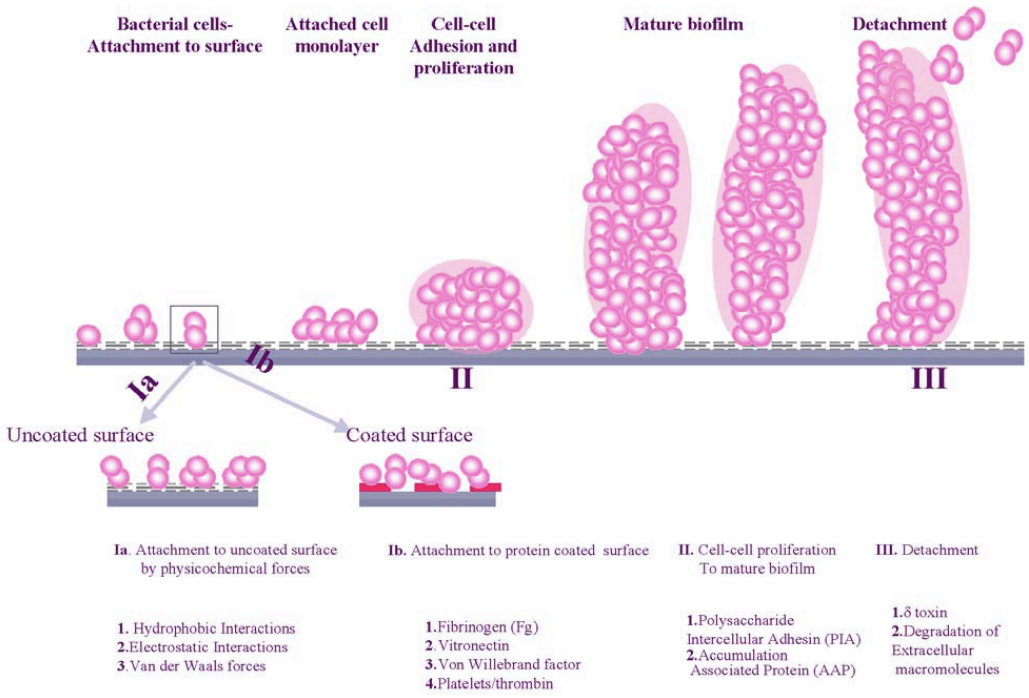

Figure 1 Schematic representation of attachment of bacteria, different formation phases of *S. ephidermidis* biofilm and the contributed microbial factors (Vuong and Otto, 2002)

The DLVO theory was proposed to apply to explain the bacterial adhesion mechanisms. When a bacterium reaches a substratum surface, physicochemical interactions between the cell and the surface can be attractive and repulsive. The attractive interaction is due to van der Waals forces while the repulsive interaction is mostly due to the negative Coulomb interactions between the electrical double layer of the cell and substratum. The net balance of attractive and repulsive forces might contribute to the adhesion of bacteria to bio-surfaces, as proposed by DLVO theory. But the DLVO theory does not take into consideration the surface properties, surface structure, molecular and cellular interactions as discussed above.

Research has shown that various factors will contribute to the complex process of bacterial adhesion. The attachment of bacteria is influenced by the environmental factors

such as the surrounding flow conditions, the presence of substances, bacterial concentration, bacteria type and the material properties. Flow conditions have been studied to show a significant role in the attachment of bacteria and it is suggested that high shear rate generally generates high detachment forces for more detachment of bacteria (less attachment of bacteria) (Katsikogianni et al., 2004).

Some bacteria such as *E. coli*, are known to have mechano-sensitive channels. Minor deformations caused by adhesion forces create membrane stress which the adhering bacteria could be aware of and will thus change from a planktonic form to biofilm phenotype (Busscher et al., 2012).

Three adhesion force regimes have been described on how bacteria respond to different adhesion forces, as shown in Fig. 2.

a. Planktonic regime. This is the regime where the adhesion forces are extremely weak that the bacteria adhered are unable to sense the change of environment. The adhered bacteria cannot notice the existence of the attaching surface so that they fail to adapt themselves from planktonic phenotype to a more viable form.
b. Interaction regime. This is also the transition or intermediate regime of bacterial adhesion forces. The phenotypic changes increase as bacteria responses more to the environment when the adhesion forces increase. The adhesion forces at interaction regime are estimated because the adhesion forces have a tendency to increase pronouncedly in the first few minutes rending an irreversible switch.
c. Lethal regime. Since the majority of bacteria strains possess a negative surface charge, whereas on positively-charged surface, adhesion forces can be found. In the lethal regime, the adhesion forces are significantly strong. On the positively-charged

substratum surface, a minimum density of positive charge is required to kill certain amount of bacteria species.

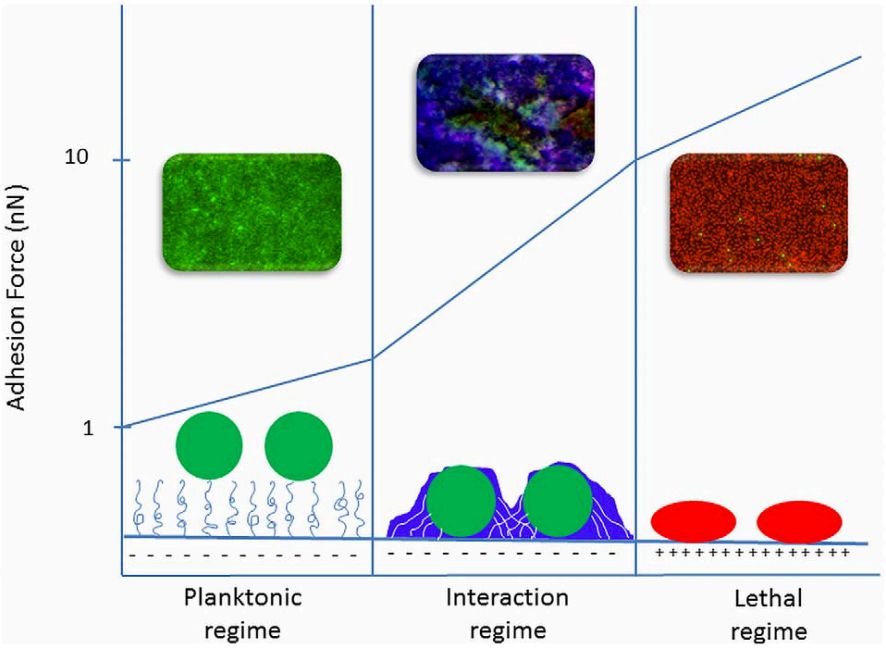

Figure 2 Three regimes of bacterial adhesion (Busscher et al., 2012)

1.4. Mathematical modeling of produce bacteria interactions

A mathematical model predicting the attachment, growth, and detachment of bacteria was proposed by De Jong et al. (2002). In milk and dairy product processing, microbial cross-contamination takes place easily on heat exchanger surfaces during heat transfer. According to De Jong et al. (2002), in thermal processing, the whole process of bacterial attachment is mediated by a complicated mixture of interactions including van der Waals forces, hydrodynamic interactions and cell-to-cell interaction, as shown in Fig. 3.

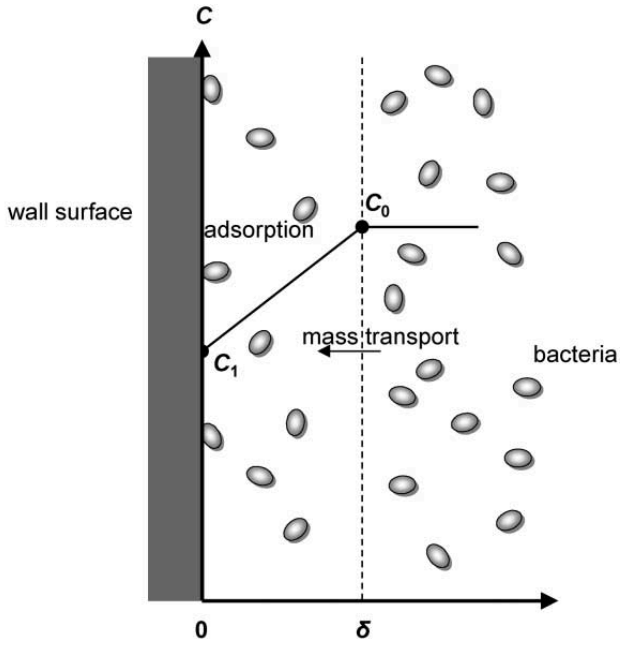

Figure 3 Heterogeneous reaction process of bacterial adsorption (De Jong et al., 2002)

The adhesion of bacteria to solid surfaces is not only a function of adhesion reaction with the solid surfaces mediated by “adsorption rate”, but also the function of mass transfer of bacteria, since the total number attached to the surface is influenced by the number of bacteria transferred to proximity of substratum surface. Two variables in the process influence the number of bacteria attached: the adsorption rate and the transfer rate of bacteria. The adsorption rate plays a more important role in bacterial adhesion in that the bacteria at the surface available for bacterial attachment are limited by adsorption rate, rather than their transfer rate. (De Jong et al., 2002).

An apparatus with a rotating disk was described by (De Jong et al., 2002). Instead of attaching an inoculated leaf on the rotating disk, the liquid in the tank was inoculated with bacteria as shown in Fig. 4. The hydrodynamics of the liquid flow along the surface of the rotating disk has been discussed by (Levich, 1963). On the bottom side of the rotating disk in the fluid, where the hydrodynamic boundary layer is, radial velocity,

angular velocity and axial velocity exist. Beyond the boundary layer near the surface, only axial velocity exists. Three regions along the surface were shown in Fig. 4. The final count of bacteria on the surface was estimated as the net accumulation of the deposition (adherence) and release of bacteria induced by shear (Aubert et al., 1993; Dickinson and Cooper, 1995). The mathematical model developed by (De Jong et al., 2002), to be applied in industrial food processing chains, shows that the contamination of the produce is affected by the growth of bacteria during processing, and the inactivation by engineering techniques.

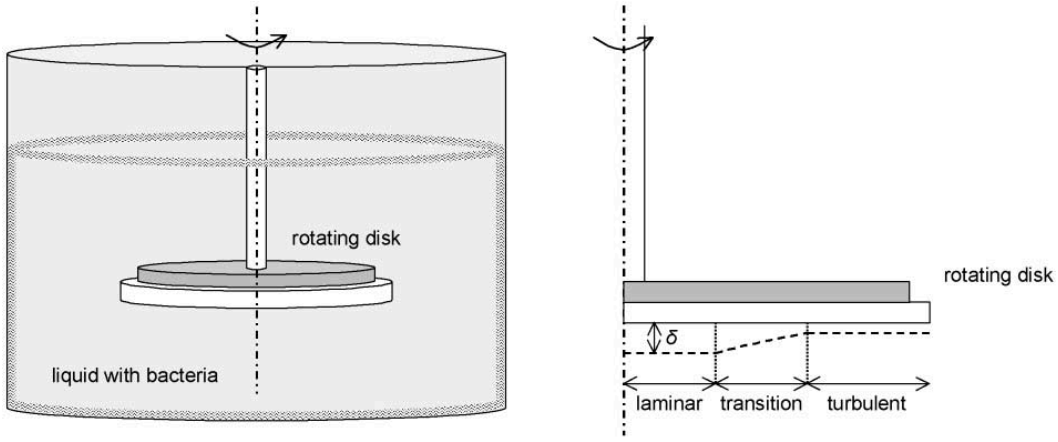

Figure 4 Schematic representation of the apparatus used for predictive model of the adherence, growth and detachment of microbes in production chains (De Jong et al., 2002)

Shear-dependent bacterial adhesion kinetics model

The deposition of bacteria onto the surface and the detachment of microorganisms are dependent on shear rate (Dickinson and Cooper, 1995). The parallel flow chamber or radial flow chamber, as shown in Fig. 5, were often used for studying shear-dependent bacterial adhesion (Busscher et al., 1992).

The radial flow chamber was used in the experiment conducted by Dickinson and Cooper (1995) to study bacterial attachment and detachment as a function of shear stress. The research studied further the intrinsic properties of bacteria that affect attachment and detachment kinetics. The attachment and detachment rate constants were predicted by a probabilistic model using data fitting. The two rate constants were found to be dependent on the bacteria type. It was found that the two rate constants are functions of bacteria to surface interactions, and the local hydrodynamic conditions on the surface instead of the global fluid conditions.

The attachment rate constant was a function of time according to Dickinson and Cooper (1995). The attachment rate constant was constant whether there was monolayer of bacteria or a multilayer of bacterial groups. The value of detachment rate constant observed using similar radial flow apparatus shifted more significantly when higher fluid flow was induced, i.e., by increasing the flow velocity, after initially attaching to the substratum surface. It was reported that higher shear stress, by adjusting the volumetric flow rate applied might be required to achieve adequate number of bacteria detachment, depending on different experimental cases (Warning and Datta, 2013). The bacteria suspended in global domain were assumed to be in homogeneous state before attaching to the surface. Once attached, different adhesion state might possibly take place and the heterogeneity of bacteria distribution existed. The probability of different bacterial cells adhering at different attachment point from the same distance should be equal (Dickinson and Cooper, 1995). Herein, to escape from the adhesion state and release from the surface, the heterogeneity of bacteria detached occurred due to the distribution of attachment points.

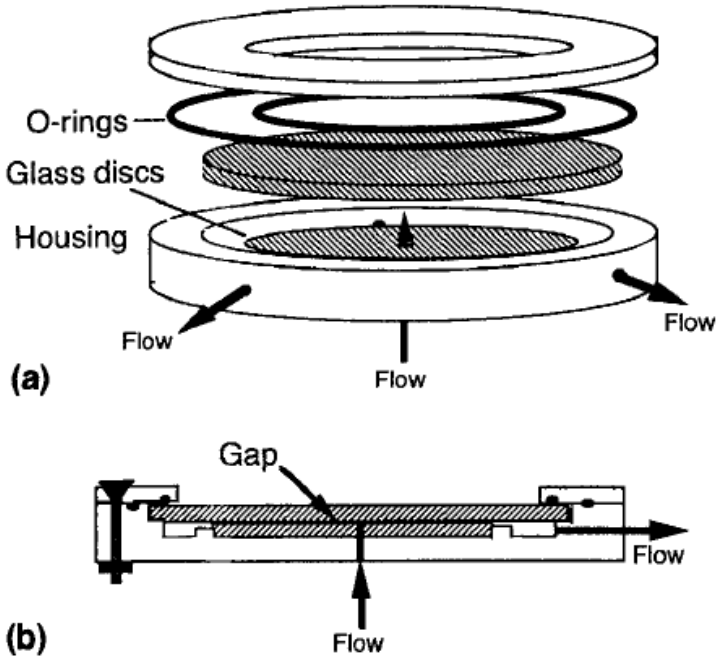

Figure 5 (a) Dismantled and (b) assembled radial-flow chamber. The Plexiglas radial-flow chamber contains the central flow inlet, several loosely stacked discs which can be easily removed, three equally spaced outlets. The flow can be collected radially in the trough through the central inlet port (Dickinson and Cooper, 1995).

Deterministic receptor-mediated cell adhesion dynamic model

One research by Hammer and Lauffenburger (1987) suggested that the adhesion of bacterial cells to a biomaterial surface was mediated by the specific binding between the cell molecules and the ligands on the complementary surface as receptors. Upon adhesion and deposition, the number of bonds were determined by the certain rate constants. The bonds form when the receptors enter the contact area, thus the total bonds formed were affected by the size of contact area and the rate of accumulation. It was noted that the

strength of bonds is also important with regards to the attachment of bacteria in that the bonds might break in response to external forces.

The dynamic "point attachment model" proposed by Hammer and Lauffenburger (1987) indicated that the adhesion of bacteria to a surface is mediated by the receptor-ligand binding and the adhesion behavior was assumed to be point-to-point interactions. The affecting factors of bacterial cell adhesion are shown in Fig. 6.

As shown in Fig. 6, within the contact area, a certain number of receptors form specific binding bonds with ligands which indicate that the size of contact area, the number and density of receptors and complementary surface ligands influence the adhesion. Moreover, external factors such as the shear torque and shear force by passing fluid flow influence receptor-mediated cell adhesion.

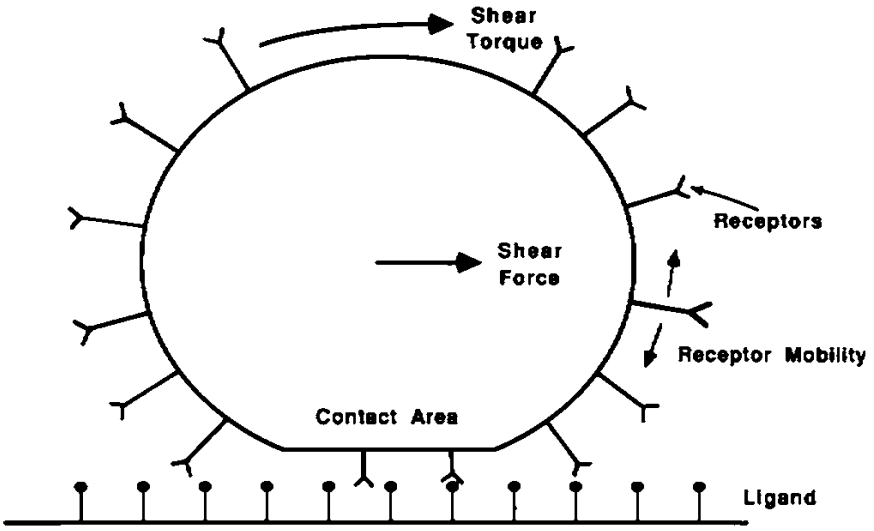

Figure 6 Schematic representation of receptor-mediated adhesion (Daniel and Lauffenburger, 1987).

The assumptions made on the mobility of cells and adhesion are shown in Fig. 7. It was assumed the contact area remained constant throughout the contact and further adhesion. Next, contact time T_c was assumed the time in which the cells overcome the external force and roll forward to distribute its bonds. There was still little amount of shear stress in the initial stage of contact, but maximum stress exerted on the cell occurred when the normal stress brought by the external torque was applied on the bacterial cell. Furthermore, the normal stress distribution was likely to be a function of position (Schmid-Schonbein et al., 1975, Evans et al., 1985) but was assumed in the dynamic theory to be equally distributed within the contact area.

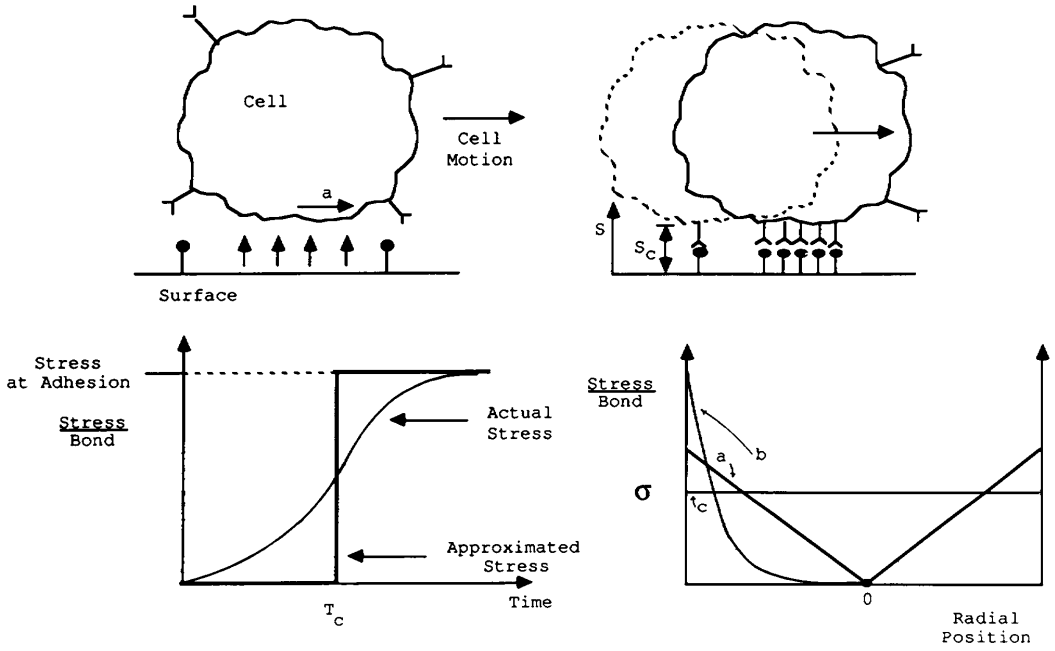

Figure 7 Schematic representation of cell motion under shear flow (top line); Contact time T_c (bottom left); Stress bond distribution along the radial position (bottom right) (Daniel and Lauffenburger, 1987)

It was proposed in this model that the contact area is a function of net accumulation of forces acting on the cell. The normal forces include the adhesion and deposition forces such as gravity or hydrodynamic forces, and other interactions such as the van der Waals interactions, electrostatic interactions, and deformational forces.

Forces and torques exerted by the bonds were calculated by the mechanical equilibrium shown in Fig. 8. As shown in the figure, the adherent cell is in equilibrium state where no external force or torque was applied on the cell. The bonds formed between the receptors and the receiving surface in the contact area act in both translational (parallel to the direction of fluid) and normal (to the cell surface) directions. The shear force F^s in the x-direction on the cell imparted by the passing fluid, is balanced by the bonding force F_x^b which acts in the opposite direction and with the same magnitude. The bonding force acting as a pulling force, imparts a torque of the magnitude $F_s R_c$ on the cell (Hammer et al., 1987). The torque $F_s R_c$ in the z-direction imparted by bonding force, along with the shear torque τ^s imparted by external fluid, must be balanced by normal stresses σ, force per bond, to resist the motion of the cell. The distance between the cell and the surface (length of lever arm of the bonds) will determine how effective the bonds are able to resist the torque on the cell.

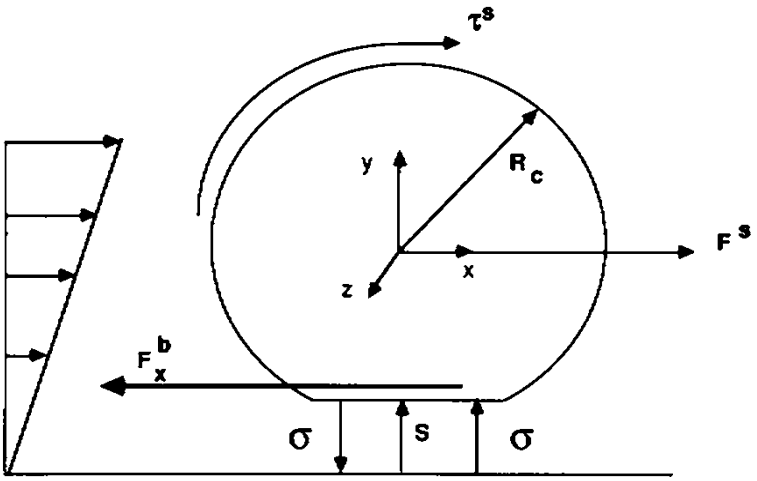

Figure 8 Schematic representation of mechanical equilibrium of adherent cell under passing flow (Daniel and Lauffenburger, 1987)

The research conducted by Cozens-Roberts and Lauffenburger (1990) extended this deterministic receptor-mediated cell adhesion kinetics model to a probabilistic model. The probabilistic model calculated the possibilities of a certain number of bonds between a cell and surface exists. Two cases were investigated: the attachment case and the detachment case. In the attachment case, the expected variance in bond formation was examined as a function of attachment time in the absence of fluid; in the detachment case, cell detachment as a function of key system parameters such as distractive fluid force and rate constants, was studied in the presence of fluid. It was found that the deviations from ideal deterministic attachment and detachment model was related to deviations in kinetics, also may result from the heterogeneities in cell properties and surface properties.

1.5.Numerical Simulation of produce washing

Parallel-flow plate chamber

A traditional method to measure the bacterial adhesion and detachment is by parallel-plate chambers (Brown and Larson, 2001). One drawback of the parallel-flow chamber is although large number of bacteria can be measured at the same time, the size of the device is relatively large to enable the microscopic measurement of adhesion behavior. Thus, there was requirement for a more detailed examination using microfluidic flow chamber. The microfluidic device allows for close observation of bacterial hydrodynamics under fluid flow at single-cell scale, schematic illustration and sizes are shown in Fig. 9.

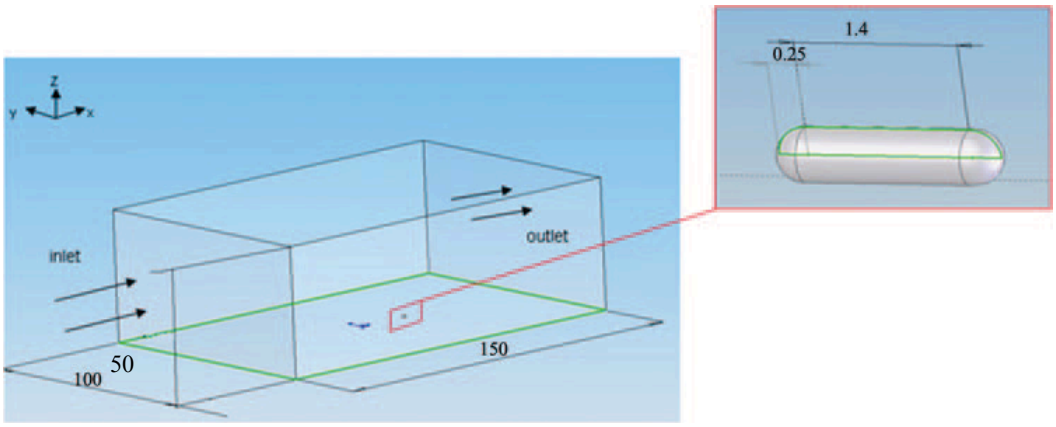

Figure 9 Schematic illustration of microfluidic flow chamber used for bacterial adhesion study. The flow was simulated using ANSYS Fluent software. As shown in this figure, dimensions of the simulation box were 100 μm wide, 150 μm long and 50 μm deep. The model bacterium attached on the bottom surface of the channel was 0.5 μm in diameter and 1.4 μm in length (De La Fuente et al., 2007)

The influence of flow conditions on cell detachment was studied by gradually increasing the flow rate. It was found that the bacteria have a tendency to slide downwards with the flow. It was also observed the bacteria can be instantly washed off by the flowing fluid. In the microfluidic flow chamber, bacteria attached on the surface were exposed to drag forces exerted by the flow. When flow rate increases, the drag force increases. The amount of drag forces required to remove the bacteria attached on the surface were dependent on the global flow, also being a function of intrinsic characteristic of bacteria (De La Fuente et al., 2007).

Microfabrication

The attachment, growth, aggregation and coaggregation of bacteria on a plant surface were discussed in the earlier section. Colonization of bacteria is a major concern in food safety of fresh produce and the effect of microstructure of produce surface is important. To study the effect of microstructure under fluid flow, a dynamic environment was investigated both numerically and experimentally by Delwiche et al. (2013) using a flow chamber.

As shown in Fig. 10, the flow chamber was designed to create certain layer of surface flow over an artificial plant surface piece. The inlet flow was distributed evenly across the channel forced by the trough at the entrance.

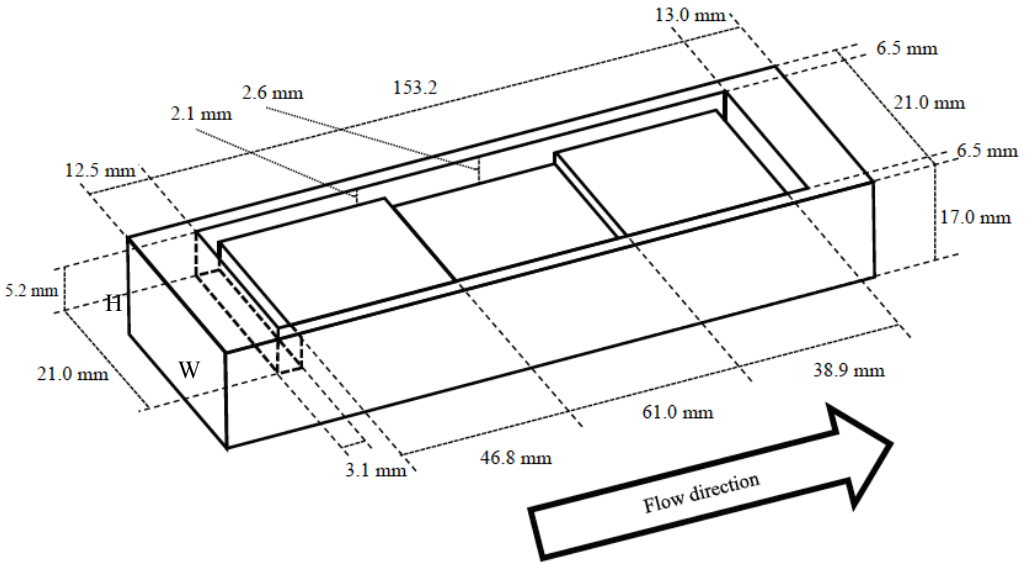

Figure 10 Diagram of the flow chamber for the study of effect of flow on microbial attachment (Delwiche et al., 2013)

Due to relatively small size of the flow chamber and low flow velocity, the flow in the micro-chamber was laminar (Reynolds number less than 1000). Reynolds number was defined as

$$\mathrm{Re} = \frac{\mathrm{v}\mathrm{D_h}}{\nu}$$

.....(1.1)

where, v is the velocity of flow (mm/s), ν is the kinematic viscosity (mm^2/s), D_h is the hydraulic diameter calculated for a rectangular channel.

$$\mathrm{D_h} = \frac{2\mathrm{HW}}{\mathrm{H} + \mathrm{W}}$$

.....(1.2)

In equation (1.2), HW in the numerator denotes the area of the chamber cross section, and the denominator (H+W) denotes half the wetted perimeter of the cross section. H is the height of channel (mm), W is the width of channel (mm), as shown in Fig. 10.

The real flow conditions resulting from rain, irrigation of plant surfaces, or post-harvest handling have been modeled to mimic the flow of liquid moving down from an inclined leaf plane (Sirinutsomboon, 2011; Delwiche et al., 2013). The average film flow velocity (v) (Bruus, 2007) is:

$$v = \frac{gh^2}{3\nu}\sin\theta \qquad \text{.....(1.3)}$$

where, h is the thickness of film (m), θ is the inclination angle (radian), g is the gravitational acceleration constant (m/s^2), ν is the kinematic viscosity (m^2/s).

The total shear stress exerted on leaf surface was calculated by:

$$\tau_w = \rho g h \sin\theta \qquad \text{.....(1.4)}$$

where, ρ is the liquid density (kg/m^3), and θ is the inclination angle (radian).

The shear stress calculated by equation (1.4) was estimated by simplified simulation of flow channel, where microstructures of the surface were not taken into account. When fluid flows over the surface, wall shear is affected by the microstructures. It was investigated that the bacterial attachment was influenced by the location around microstructures. The wall shear stress was calculated and estimated numerically using computational fluid dynamics model by (ANSYS, version 12.1, Canonsburg, PA, Delwiche et al., 2013). The software could take into account the microstructure geometry thus better estimate shear stresses around the microstructures. Higher shear stresses were

observed at greater flow. The wall shear stress values calculated by computational fluid dynamics model were in the range of 30 mPa to 2400 mPa when different flow rates (20, 100, and 500 mL/min) were applied continuously (Delwiche et al., 2013).

Dynamic model of receptor-mediated specific adhesion of bacteria under uniform shear flow

Bacterial cell adhesion in viscous shear flow is mediated by specific receptor-ligand binding (Wang and Bryers, 1997). In this dynamic model, the attachment, detachment and growth of attached bacteria were modeled in a reactor with uniform shear flow. This mathematical dynamic model assumed the bacterial cells as ideal spherical particles, which were covered with uniformly distributed spring-like receptors. The attachment, detachment and growth of attached bacteria were mediated and controlled by receptor-ligand binding. Only receptors within the contact area were assumed to form the specific bonds with ligands and thus mediate adhesion.

Numerical analysis was conducted by solving a set of non-linear ordinary differential equations (ODEs) using 4^{th} order Runge-Kutta methods (James et al., 1985). The ODE equation set contains three equations including three variables: the net number of ligand-bonded cells per surface area (B), the total number of suspended cells in bulk liquid (X) and growth-limiting substrate concentration (S).

The non-linear ODE equations derived by Wang and Bryers (1997) were modified and discussed in section 2.4.

Flow chamber model

Produce washing conditions play an important role on food safety. A lab-scale experiment was conducted to investigate the effect of flow conditions on microbial reductions. The model proposed by (Wang et al., 2007) focused on the effect of fluid dynamics on reduction of *E.coli* O157:H7.

The device used by (Wang et al., 2007) to study the effect of fluid velocity is shown in Fig. 11.

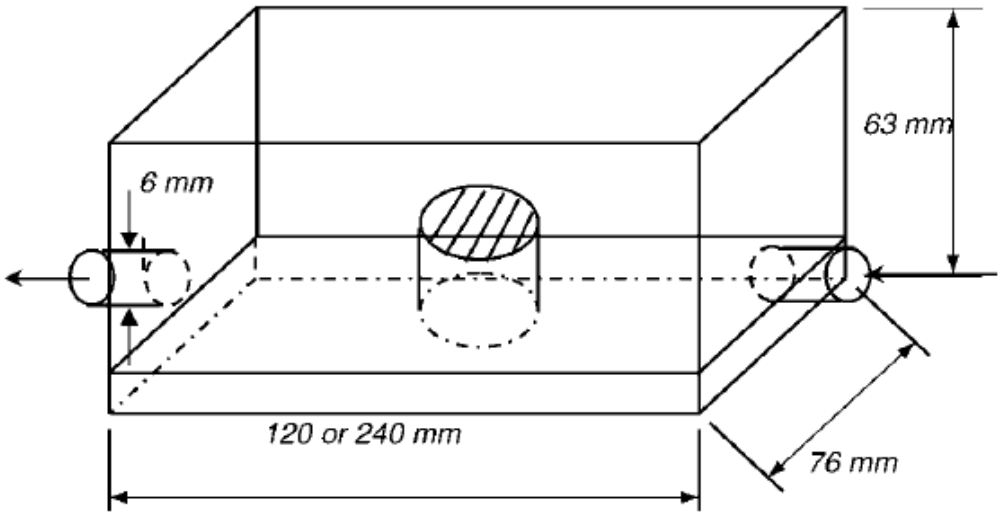

Figure 11 Schematic diagram of 2 flow-through washing chamber to study the effect of fluid velocity on the reduction of *E. coli* O157:H7 (Wang et al., 2007)

Two similar flow chambers which differ in the length (120 mm and 240 mm) were used in the experiments; the other dimensions are specified in Fig. 11, which differed in length. The fluid velocity was changed by adjusting the volumetric velocity of entering flow. The sample was mounted on the sample holder on the center bottom of the chamber.

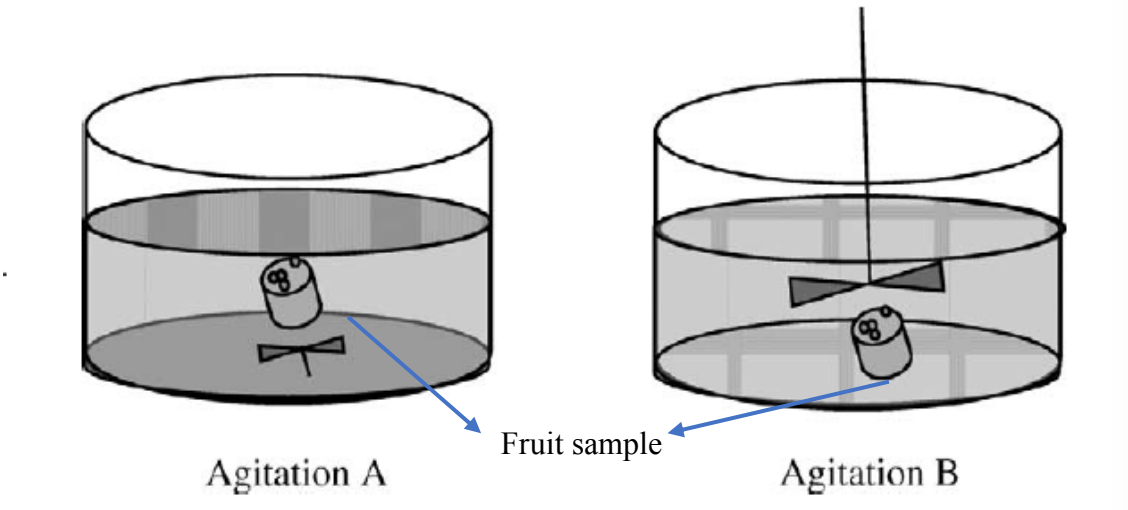

Figure 12 Schematic diagram of agitation device (Wang et al., 2007)

The schematic drawings of two agitation devices are shown in Fig. 12. The two devices differed in the location of the agitator. In one case (Fig. 12A), the agitator was below the fruit sample whereas in the second case (Fig. 12B), the agitator was above the fruit sample. This difference in the setup induced the difference in the fluid flow field. Approximately 2.5 log CFU/cm^2 and 2.3 log CFU/cm^2 reduction of *E. coli* O157:H7 were observed on cantaloupe rind and cup apples, respectively, in the flow-through chamber (Fig. 11), when the fluid velocity increased from 0 m/min to 0.8 m/min, within processing time of 3 min. 1.2 log CFU/cm^2 reduction of bacteria was achieved in agitation mode A; while 0.8 log CFU/cm^2 of reduction was achieved at 3 min in agitation mode B where the agitator was above the sample.

In static mode when no flow and no shear were applied on produce surface, no significant reduction of *E. coli* O 157:H7 was observed. When no external shear force was applied, removal of bacteria was not effectively enhanced by merely increasing washing time. Experiments conducted by Wang et al. (2007) revealed that extending

washing time was only effective in the first 2-3 minutes of washing. These experiments results indicated that the fluid flow and shear field have great impact on the removal of bacteria.

Cross-contamination pilot plant washer model

Under commercial processing conditions, processing conditions are a vital step to maintain and enhance the food safety of fresh produce. Wash water is the most favorable medium for the potential transfer and growth of bacteria. Thus, a sanitizing agent in wash water is quite critical in prevention of cross-contamination during processing.

A pilot plant scale evaluation of produce washing was conducted by (Luo et al., 2012). The transfer and inactivation of pathogens were affected by the fluid flow conditions of wash water, and by the concentration and activity of chemical sanitizers. The natural decay and deactivation of chlorine sanitizer by reacting with organic matter in wash water, such as debris, soil and plant exudates brought by the produce into washer system, will deteriorate the wash water quality. The deterioration of wash water quality further affects the efficacy of sanitizing agents in inactivating the pathogens in wash water, which results in rapid depletion of available chlorine. The disinfection of pathogens is limited due to shortage of free chlorine. Therefore, the inspection of chlorine activity and the periodic replenishing of chlorine is necessary in the industrialized processing system. The pilot plant scale experiment was conducted to study the cases in a commercial environment as shown in Fig. 13.

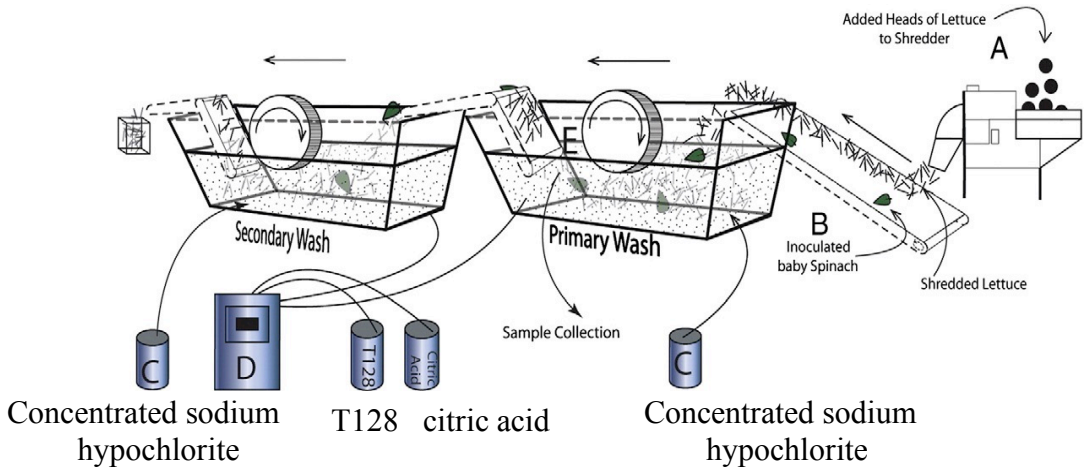

Figure 13 Schematic diagram of the pilot plant wash system including produce and chemical inputs and flow (Luo et al., 2012) C: sanitizing agent used in pilot plant washing, concentrated sodium hypochlorite D: replenish of T128 or citric acid to adjust the pH of wash water

The pilot plant cross-contamination experiment was designed and conducted by Munther et al. (2014). In this pilot plant scale washer system, un-inoculated lettuce leaves were shredded and automatically transported by the conveyer belt to be distributed into the washing system. Some inoculated fresh-harvested baby spinach leaves were manually added onto the conveyer belt, near to the shredded lettuce leaves. There was no physical contact between two types of the fresh produce. In the primary washing step, concentrated chlorine hypochlorite was added manually and periodically. In the following secondary wash tank, T128 (novel developed chemical mixture functioned to stabilize the hypochlorous acid in wash water of high organic load, Lemons and Taylor Fresh Food, Inc., 2009) and citric acid were added automatically. Water, lettuce leaves

and baby spinach leaves in the primary tank were periodically taken out from the upper water surface to evaluate the change in water quality, and the survival of pathogens on leaf surfaces after inactivation treatment.

To quantify the cross-contamination dynamics during the produce processing, a mathematical model was developed by Munther et al. (2014). Two dynamics were discussed in the mathematical model. The chlorine dynamics in the wash tank and the cross-contamination dynamics in the wash tank.

As for the chlorine dynamics, the exact level of free chlorine was difficult to predict (Luo et al., 2012) as it was affected by various factors. However, the organic matters which influenced the efficacy of chlorine in water could be measured and quantified. In this mathematical model, the rate of increase of chemical oxygen demand (COD) was constant. The change of free chlorine with time was a function of the natural decay of free chlorine, the depletion of free chlorine and the periodic addition of chlorine into the wash tank.

As for the cross-contamination dynamics in the wash tank, mathematical equations were developed to quantify the concentration of pathogens during processing. The concentration of pathogens in water is affected by the amount of pathogen transferred from baby spinach, the amount of pathogen transferred and attached on the produce surface and the amount of suspended pathogen inactivated by chlorine. The concentration of pathogens on lettuce is influenced by pathogens attached/bound to lettuce, pathogens inactivated by free chlorine, and pathogens available in the wash tank.

The parameters used in the mathematical equations were obtained from experimental data (Luo et al., 2012) in a pilot plant scale equipment. Some of the parameters were

numerically obtained by data fitting in MATLAB® R2010a (The Mathworks, Inc.). Direct transmission of bacteria from produce to produce was not considered in this dynamic model (Munther et al., 2014).

The mathematical model as well as the experimental data helped assess the cross-contamination in processing environments, as well as the efficacy of associated wash-cycle protocols (Munther et al., 2014). This mathematical model was further discussed and referred in section 4, in the improved ODE model where sanitizing agents were considered.

1.6. Rationale

Due to an increase in health awareness, there is more demand for fresh produce. The consumption of ready-to-eat food has increased over the last few years. Cases of major outbreaks related to fresh produce have also been rising. Since most of the fresh produce is consumed raw or without any processing/killing step to inactivate harmful pathogenic microorganisms before consumption, food safety of these raw/fresh produce is of prime concern.

Physical methods and chemical methods are usually taken to enhance the removal and inactivation of bacteria during processing. Many of the chemical treatments are highly effective in reducing microbial load in wash water, while have limited effects on bacterial removal from produce surface (Gil et al., 2009). Therefore, this research focused on the effects of physical force (shear stress) on the removal of bacteria. Experimental (by UC Davis team) and numerical approaches were adopted in this study.

Increasing cases of foodborne illnesses resulted from fresh produce in recent years have prompted the industry to consider new practices aimed at reducing the risks of pathogenic microbial contamination on the produce. The presence of organic matter in wash water not only decreases the efficacy of sanitizers to inactivate microorganisms, but also has the potential to transfer contamination to produce. This research also aimed at numerical and mathematical modeling of the transfer of bacteria from inoculated organic particles to uninoculated leaves during the washing of produce.

1.7. Objectives

The objectives of this study were:

a) Numerical simulation of the modified one-rod benchtop device used for detachment study, and numerical simulation of the experimental setup for bacterial transfer and attachment study. Calculate the shear stress values under different flow conditions.
b) Study the effect of shear stress on bacterial removal and attachment by comparing numerical and experimental results (by UC Davis team).
c) Mathematical model of microbial cross-contamination during produce washing, with/without chemical sanitizers in wash water.

The results from this research can serve a starting point for the future guidelines of the design of fresh produce washer system.

2. EXPERIMENTS

In this section, experimental devices used for bacteria detachment study and bacteria transfer and attachment study were described. The benchtop scale devices were designed and fabricated for experiments, and the dimensions were later used in numerical simulations which are discussed in section 3.

2.1. Experimental setup

The experimental benchtop device designed and fabricated (at UC Davis) is shown in Fig. 14, Fig. 15, and Fig. 16. The general goal of this experimental study was to expose a single leaf surface to the continuous shear stress created by the rotation. The shear stress varied along the diameter of the leaf surface and the level of shear stress created was controlled by mediating the rotating speed in this benchtop scale device. Materials used for fabrication were purchased from McMaster-Carr (Robbinsville, NJ, USA). In the detachment study conducted by Dr. Nitin's group at UC Davis, where single-phase model applied, the disk was connected with four rods and the rotation was driven by the motor, as shown in Fig. 15. Water was filled up above the top surface of the disk. A 3 cm diameter leaf sample was mounted at the bottom of rotating disk using a double-sided tape, as shown in Fig. 14. Rotational speeds of 100 rev/min and 200 rev/min were selected.

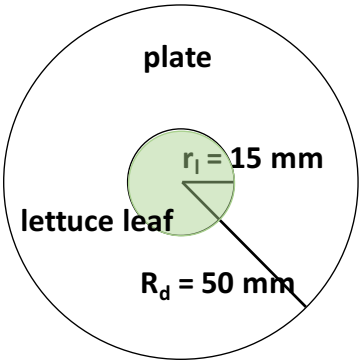

Figure 14 Diagram of mounted leaf on the central bottom of rotating disk

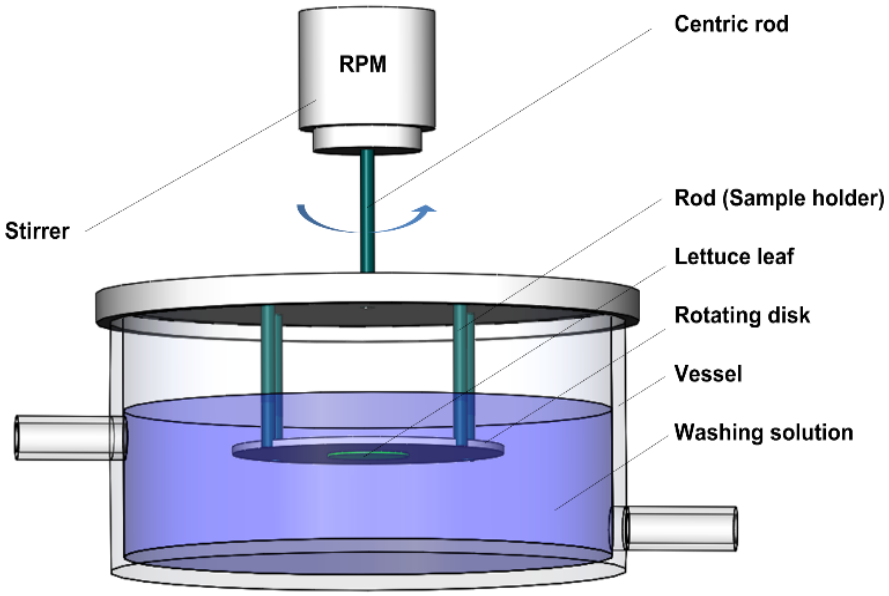

Figure 15 Experimental setup for bacterial detachment study (UC Davis)

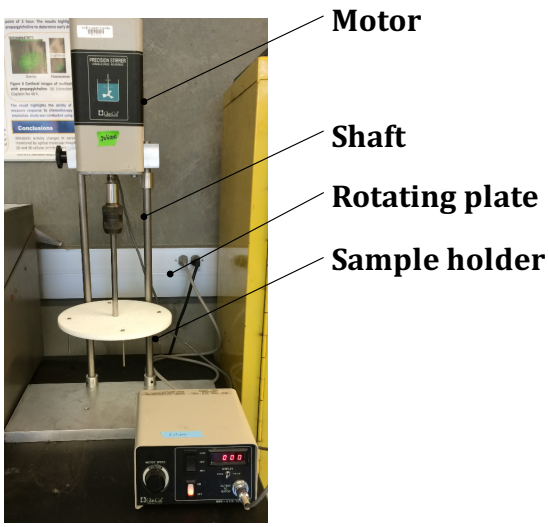

Figure 16 Experimental setup at Dr. Nitin's lab, UC Davis, for bacterial attachment study

In the attachment study involving glass beads, one rod instead of four rods was used in both the experiment as shown in Fig. 16, and numerical simulation. The central rod was affixed to a polyethylene disk. This improvement in the experimental setup was to stabilize the flow induced, and to better control the range of shear stress created. Corresponding to the first experiment, rotating speeds of 100 rev/min and 200 rev/min were used. The rotation of disk resulted in the gradient in both the velocity and shear stress on the leaf surface.

2.2. Flow regime

Usually Reynolds number, a dimensionless parameter is used for determining whether flow is laminar or turbulent. For the experimental apparatus used in this study, there is no criteria based on Reynolds number that can be used determine the flow regime.

Therefore, experiments were conducted to visualize the flow characteristics of in experimental set up, so that the flow regime could be determined.

A dye was carefully injected into the liquid of the tank using a thin pipette, after the flow induced by the rotating disk was stable. At 100 rev/min, dye erratically spread along radial, rotational and axial directions. Same experiments were also conducted at 200 rev/min. It was concluded based on visual observations that the flow induced by rotating speed 100 rev/min and 200 rev/min was turbulent. Thus, k-ε turbulent module in COMSOL® was used in numerical simulation for our study.

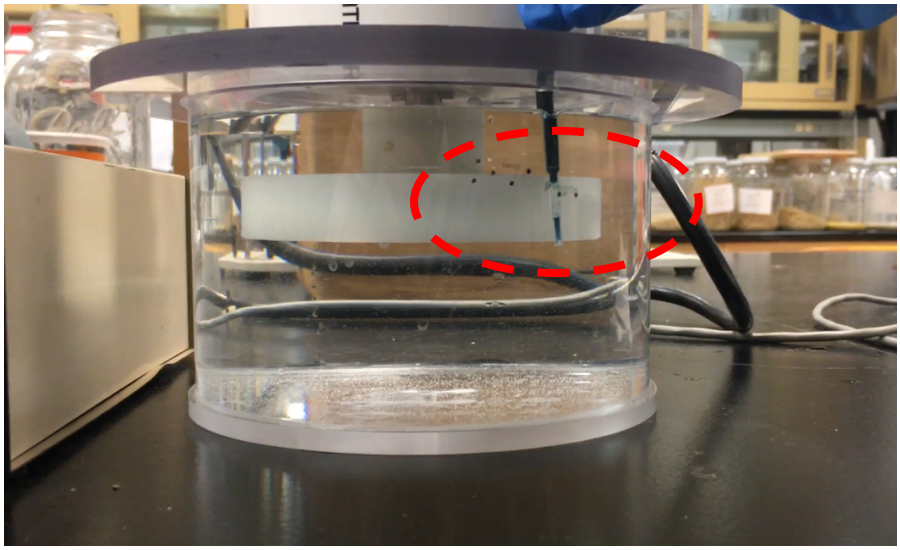

Figure 17 Flow regime induced by rotation in the benchtop device, where the dotted red line shows the injected tube and color dye

3. MATHEMATICAL MODELING

3.1. Flow induced by a spinning disk without suspended particles

To understand the effect of shear stress on detachment of bacteria from a produce surface to wash water, a benchtop scale device with a rotating disk attached to the rod, immersed in a water tank was used for both experiments and numerical simulations. The flow was induced by the rotation of the disk. A simple laminar flow system was studied to start with.

3.1.1. Geometry

3.1.1.1. Laminar flow system

In the laminar flow system, the laminar flow field was created when a disk was rotated in a large outer cylinder containing a liquid (water). The geometry consisted of a hollow cylinder filled with water, where a disk mounted on the bottom center was rotated at given rotational speed, as shown in Fig. 18b. The radius of the outer cylinder was significantly larger than the radius of the rotating disk, so that it could be regarded as an almost infinite medium with a rotating disk at the center, as shown in Fig. 18a. It was also assumed that flow was axisymmetric with a swirl. Analytical solution for this flow problem is given by Schlichting (1979).

a

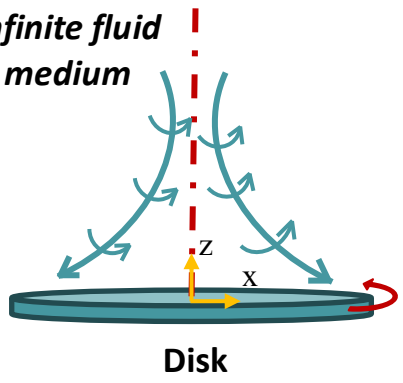

b

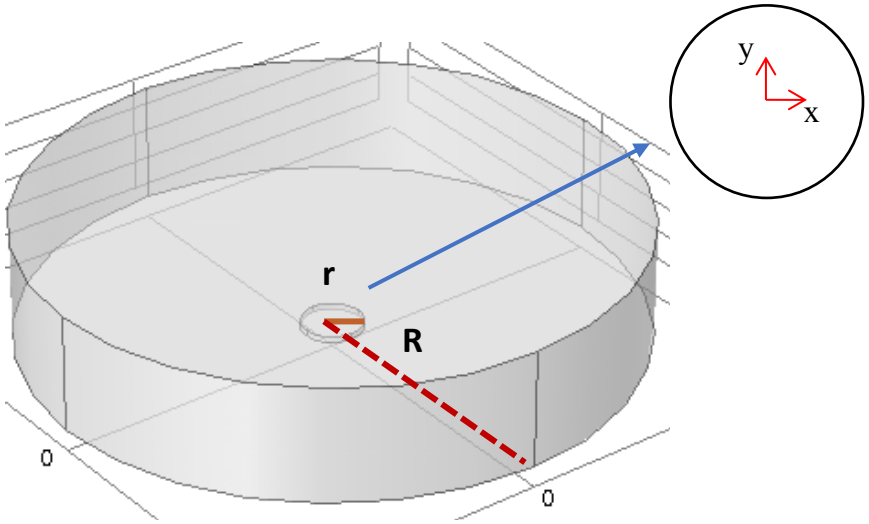

Figure 18 a. Schematic diagram of disk rotating in an infinite medium (used for analytical solutions) b. Geometry of the flow system used in numerical simulation

Geometry of the benchtop scale device

To study the effect of shear stress on the detachment of bacteria, a benchtop scale device was used (at UC Davis) for experiments. The simulation was carried out for a benchtop device which had a cylindrical tank containing a central rotating disk connected to a central rod. The geometry used for numerical simulation was slightly different from the one used for experiments. In the experimental benchtop device, there were four rods used to stabilize the rotation, shown in Fig. 19a. In the numerical simulation, one rod at

the center, instead of four off centric but symmetrically positioned rods, was used. The reasons to reduce the number of rods were: to simplify the geometry and to reduce the complexity of numerical simulation. It was found that the number of rods did not affect the final reduction of bacteria, on the bottom surface of the disk; similar bacterial detachment results were achieved by UC Davis (results not included here) in the experiments.

In the numerical simulation, it was assumed that one piece of leaf was attached to the bottom of the rotating disk. In the experiments carried out at UC Davis, the leaf was inoculated with *E. coli* O157:H7-*lux* and the cylindrical tank was filled with clean water to study the bacterial detachment by the effect of shear stress.

For numerical purposes, since the whole geometry is rotationally symmetric as shown in Fig. 19b, instead of a full 3D geometry, the numerical simulations were implemented in a radial cross section of the cylinder as shown in Figs. 19c and 19d. All three components of velocity were considered. Implementation in a 2D-symmetrical environment reduced the complexity of computation and saved computational time.

a

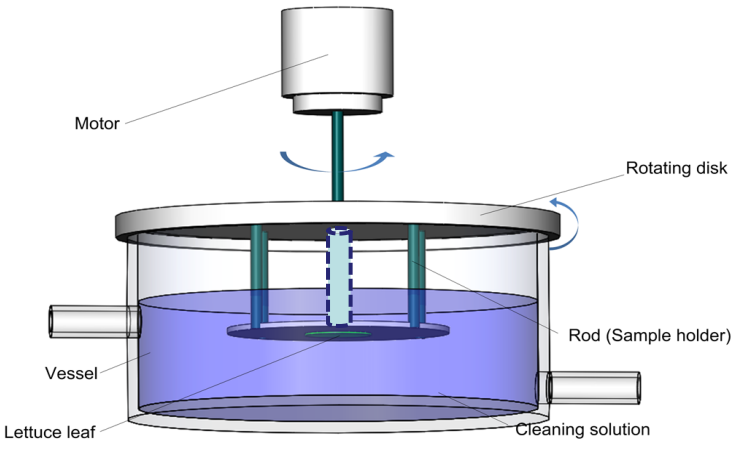

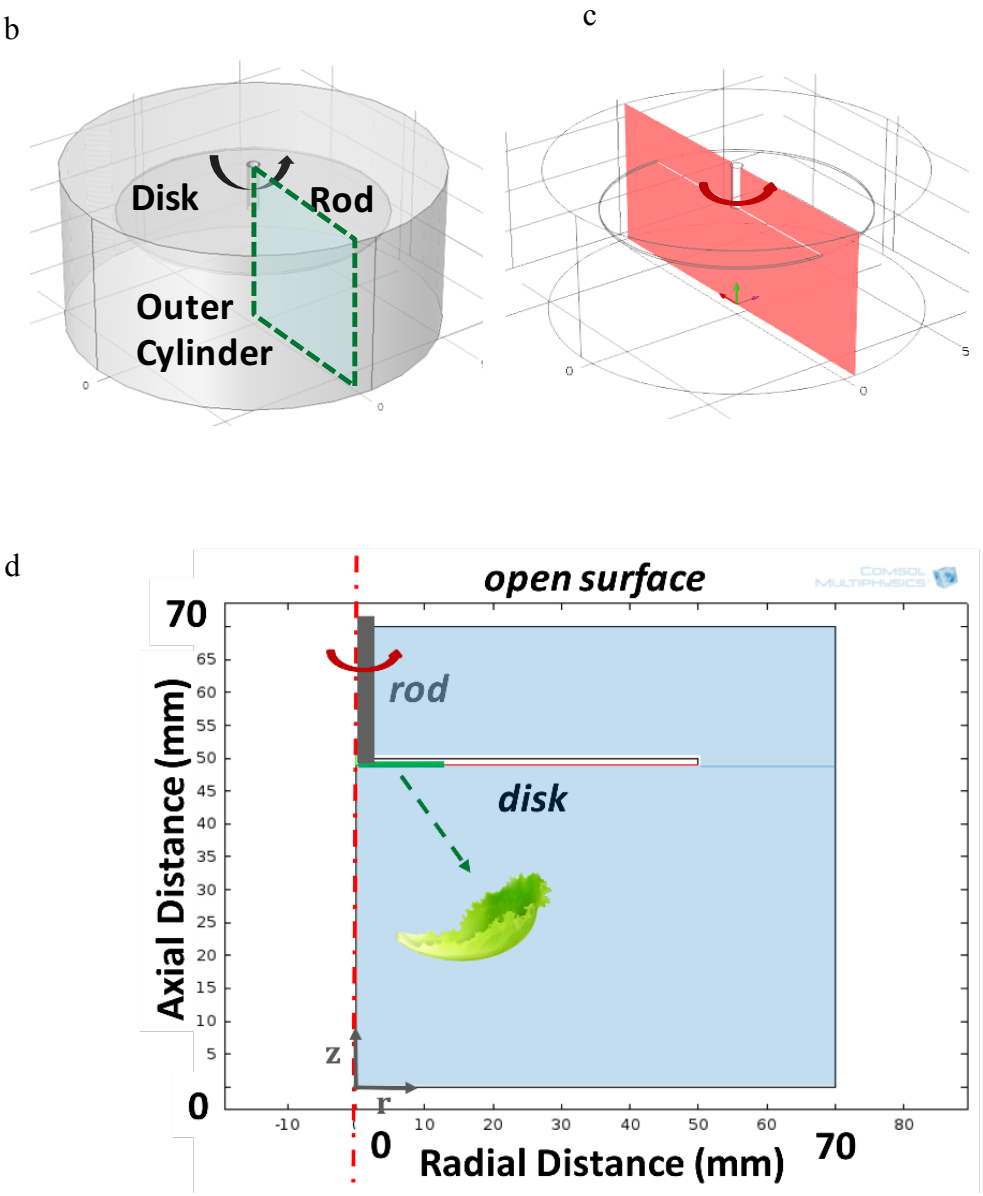

Figure 19 a. Benchtop device with 4-rods used for experiment, and the simplified central 1-rod (dotted line) b. 3D numerical geometry c. 2D radial cross section highlighted in red d. Half of the radial cross section, where the central rod and rotating disk were marked. The leaf was mounted on the lower center as shown in diagram, the radius of the leaf was highlighted in green.

3.1.2. Boundary conditions

3.1.2.1. Laminar flow system

Governing equations

The problem was solved in steady state. The governing equations are the Navier-Stokes equation for conservation of momentum and continuity equation for conservation of mass, which is further explained in section 3.1.2.2 to simulate the benchtop device.

Boundary conditions

In the laminar flow system discussed in section 3.1.1.1., shown in Fig. 18b, dimensions of the rotating disk and the outer cylinder were:

Radius of the disk: r_d = 5 cm; Thickness of the disk: h_d = 1 cm;

Radius of the outer cylinder: R = 150 cm; Height of the outer cylinder: H = 60 cm.

In order to approximate an infinite domain, a finite numerical simulation domain was used. The ratio R/r_d was varied over a broad range. It was found that the computed shear stress values not change for values of $R/r_d > 20$. Numerical results are shown in Fig. 20.

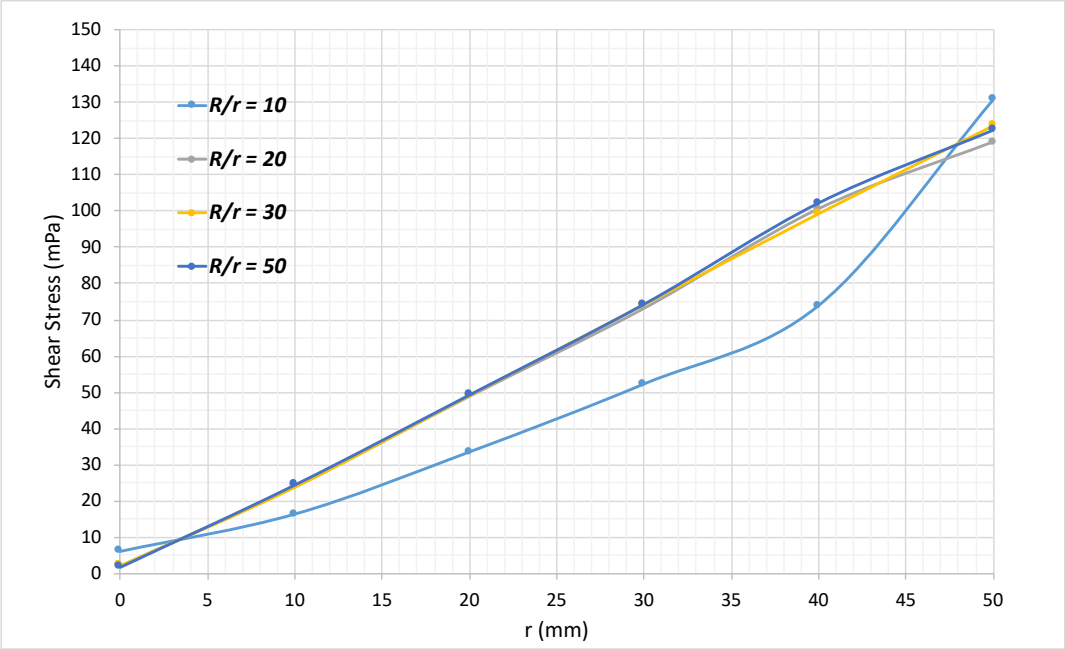

Figure 20 Numerically computed shear stress results with varied R/r ratio (10, 20, 30, and 50) in a laminar flow system as shown in Fig. 14

The Reynolds number was calculated using the equation below (Schlichting, 1979):

$$\mathrm{Re} = \frac{r^2 \omega}{\nu} \qquad \text{.....(3.1)}$$

where, r is the radius of disk rotated (m); ω is the angular velocity of the rotating disk (rad/s); ν is the kinematic velocity (m^2/s). According to Schlichting (1979), when Re < 3×10^5, the flow is in laminar region. However, this criterion is for disk rotating at the fluid at rest. According to others (Albert et al., 1993, De Jong et al., 2001, Warning and Datta, 2012), in a disk rotating system, when Re < 50000, the flow is in laminar region. In this research, the input rotating speed (N) was 10 rev/min, the angular velocity was calculated by: $\omega = 2\pi N/60$, where N was the rotating speed. Kinematic viscosity ν was

10^{-5} m^2/s. The Reynolds number calculated was 13, which is in the laminar range. Thus, in this system, laminar flow module was assumed.

A commercial finite element based computational software COMSOL® Multiphysics (Version 5.2a, COMSOL Inc., Burlington, MA) was used to numerically simulate the flow field and to calculate the shear stress values along the radius of the rotating disk, in the laminar flow system. The angular velocity of the disk was ω (rad/s). Velocity field of the rotating disk included components in all three directions: input velocity in x-direction $v_x = -\omega \cdot y$, input velocity in y-direction: $v_y = \omega \cdot x$, in x-y coordinate system; no input velocity was in the axial direction, as shown in Fig. 18a.

Material properties

The cylindrical tank was assumed go be filled with water. The density of water was 1000 kg/m^3, and the viscosity of water is 10^{-3} Pa·s. Water is Newtonian fluid. The shear stress values along the radius was computed by multiplying total shear rate and the dynamic viscosity of water, since it is laminar flow of a Newtonian fluid.

$$\tau = \gamma \cdot \mu \qquad \text{.....(3.2)}$$

where, τ is the shear stress (Pa), γ is the shear rate (1/s), μ is the dynamic viscosity (Pa.s).

3.1.2.2. Flow induced by a spinning disk in the benchtop device

Governing equations

The problem was solved in steady state. The governing equations are **the Navier-Stokes equation** for conservation of momentum and continuity equation for conservation of mass, which are:

$$\rho\frac{\partial \boldsymbol{u}}{\partial t} + \rho(\boldsymbol{u}\cdot\nabla)\boldsymbol{u} = \nabla\cdot[-p\boldsymbol{I} + \mu(\nabla\boldsymbol{u} + (\nabla\boldsymbol{u})^T)] + \boldsymbol{F}$$

.....(3.3)

$$\nabla\cdot\mathbf{u} = 0$$

.....(3.4)

in equation (3.3), **u** denotes the velocity vectors (m/s), ρ denotes the density (kg/m^3), ∇ is the gradient operator ($\nabla = \partial_x i + \partial_y j + \partial_z k$), μ denotes the viscosity (Pa·s), p denotes the fluid pressure (Pa), F denotes the body force per unit volume (N m^{-3}).

The Navier-Stokes equations describe the flow of fluid. Equation (3.3) **is** valid for flow of incompressible, Newtonian fluids. For incompressible fluid flow, the divergence of the velocity field u is zero. Thus, in equation (3.4), ∇·u=0. Once the flow has become turbulent, all quantities fluctuate in time and space.

The k-ε model is one of the most used turbulence models for applications (COMSOL® 5.2a CFD Module Users Guide). The k-ε turbulence model uses two additional transport equations and two dependent variables, besides the Navier-Stokes equations: the turbulent kinetic energy k, and the turbulent dissipation rate ε.

The transport equation for k is:

$$\rho\frac{\partial k}{\partial t}+\rho\mathbf{u}\cdot\nabla k=\nabla\cdot\left(\left(\mu+\frac{\mu_T}{\sigma_k}\right)\nabla k\right)+P_k-\rho\varepsilon$$

.....(3.5)

where ρ is the density (kg/m^3), k as the turbulent kinetic energy, u is the velocity (m/s), μ is the dynamic viscosity (Pa·s), μ_T is the turbulent viscosity which is modeled as:

$$\mu_T=\rho C_\mu\frac{k^2}{\varepsilon}$$

.....(3.6)

In equation (6), C_μ is a model constant. In equation (5), P_k is called as the production term and it given by:

$$P_k=\mu_T\left(\nabla\boldsymbol{u}:(\nabla\boldsymbol{u}+(\nabla\boldsymbol{u})^T)-\frac{2}{3}(\nabla\cdot\boldsymbol{u})^2\right)-\frac{2}{3}\rho k\nabla\cdot\boldsymbol{u}$$

.....(3.7)

The transport equation for ε is:

$$\rho\frac{\partial\varepsilon}{\partial t}+\rho\mathbf{u}\cdot\nabla\varepsilon=\nabla\cdot\left(\left(\mu+\frac{\mu_T}{\sigma_\varepsilon}\right)\nabla\varepsilon\right)+C_{\varepsilon1}\frac{\varepsilon}{k}P_k-C_{\varepsilon2}\rho\frac{\varepsilon^2}{k}$$

.....(3.8)

The model constants in equation (3.5), (3.6) and (3.8) were determined from experimental data D.C. Wilcox, *Turbulence Modeling for CFD*, 1998) and the values are listed in Table. 1.

Table 1 Model constants used for transport equations for k and ε (D.C. Wilcox, 1998)

Model Constant	Value
C_μ	0.09
$C_{\varepsilon 1}$	1.44
$C_{\varepsilon 2}$	1.92
σ_k	1.0
σ_ε	1.3

Boundary conditions

As discussed in the earlier section, the numerical benchtop device models a rotating disk in a rotationally symmetric cylindrical tank. The whole geometry is axisymmetric, it was numerically modeled as a 2D cross section with all three velocity components included.

Since no technique was available to directly measure the Reynolds number of the benchtop system discussed in section 3.1.1.2., experiments were carried out to observe the flow pattern, which was discussed in section 2.1. The flow was observed to be in a turbulent regime, when the disk was rotated at 100 rev/min and 200 rev/min. To include the velocity component in the vertical z direction, swirl flow was used. Numerical simulation was solved in 2D axisymmetric using the turbulent k-ε model with swirl flow.

The radial cross section solved for numerical simulation is shown in Fig. 21, with dimensions indicated in the figure. The dimensions used in the simulation correspond to the experimental apparatus at UC Davis. The dimensions of the rod were: radius (r_r) = 2.4 mm, height (h_r) = 20 mm; the dimensions of the rotating disk were: radius (r_d) = 50 mm,

height (h_d) = 1 mm; the dimensions of the outer cylinder (flow domain): radius (R) = 70 mm, height (H) = 70 mm. The radius of the leaf mounted at the bottom of the rotating disk was 15 mm.

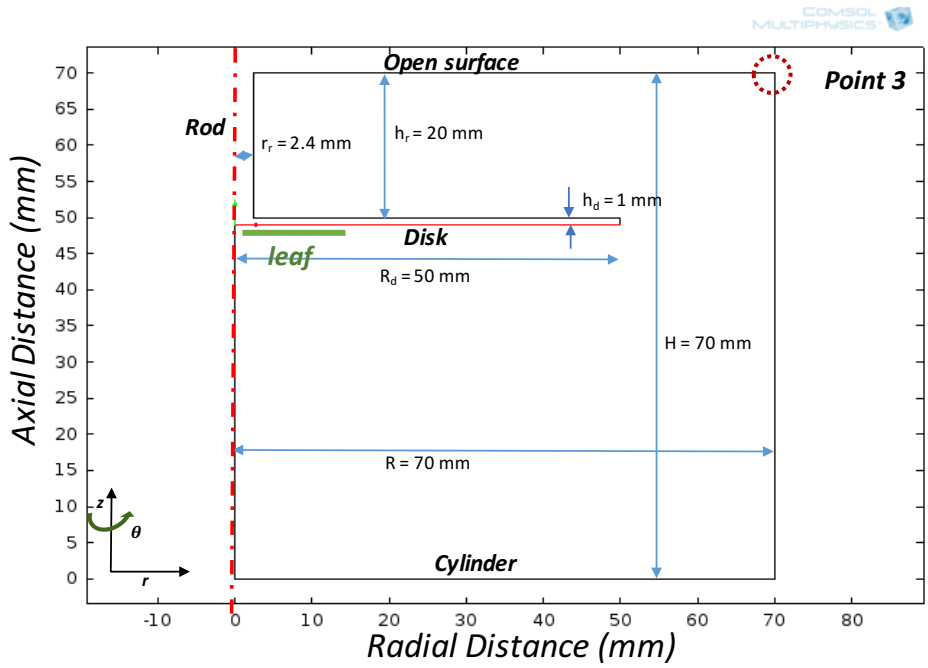

Figure 21 Dimension of the benchtop device in single-phase turbulent flow model using COMSOL®, rod and rotating disk was marked in the diagram; attached leaf as the green highlighted line

The boundary conditions used in COMSOL® simulation were:

a. Sliding wall for the rod and connected rotating disk. The sliding wall boundary conditions were used to specify the velocity. $v_r = v_z = 0$ m/s and $v_\theta = r \cdot \omega$ m/s, where $\omega = 2\pi N/60$, is the angular velocity (rad/s), N is the input rotating speed (rev/min).

b. No slip boundary condition was applied for all the boundaries representing the cylindrical outer surfaces. No slip boundary condition at the cylinder implies that all velocity components equal to zero: $\mathbf{u} = (0,0,0)$ ($v_r = v_z = v_\theta = 0$ m/s).

c. Axisymmetry boundary condition applied at the centerline which corresponds to the axis of rotation. The axisymmetry boundary condition allows flow to exist in the azimuthal direction, however, the radial velocity along the centerline is zero: $v_r = 0$ m/s.

d. Symmetry boundary condition applied on the top surface of the geometry, which is the free water surface, where velocity on the top surface $v_z = 0$ m/s, and shear stress $\tau = 0$ Pa.

e. Point pressure constraint feature was added and applied at one point of the geometry, since it was not possible to specify a pressure level using any boundary condition as an outlet. The gage pressure was set as zero at point 3 specified in Fig. 21**.**

Material property

The benchtop device was filled with water. The properties of water were used: density $\rho = 1000$ kg/m^3, viscosity $\mu = 0.001$ Pa·s. The whole geometry was solved for fluid domain only, thus the material of the rotating disk and the rod were not defined.

Mesh and Time Step

The simulation domain was divided into meshes (grids) created for computational purposes using the built-in mesh generating features in COMSOL® Multiphysics. In 2D axisymmetric model, triangular mesh was generated in the computational domain.

The results were obtained by numerically solving the governing equations using finite elements (mesh consisting of triangular mesh). The computational results were improved by refining the mesh size. Mesh size was gradually decreased until the final

computational results were independent of the mesh size. The triangular mesh used for computation is shown in Fig. 22. Fig. 23 represented the final mesh after adaptive mesh refinement analysis, to adapt the accuracy of the solution within certain turbulent regions of the domain.

The final computational mesh had 92320 elements. The convergence criterion was set to 10^{-6} as the relative tolerance on velocity. It took 6 iterations to reach convergence. The total computational time required was 75 min on a DELL Inc. workstation with Intel® processor with 12GB RAM.

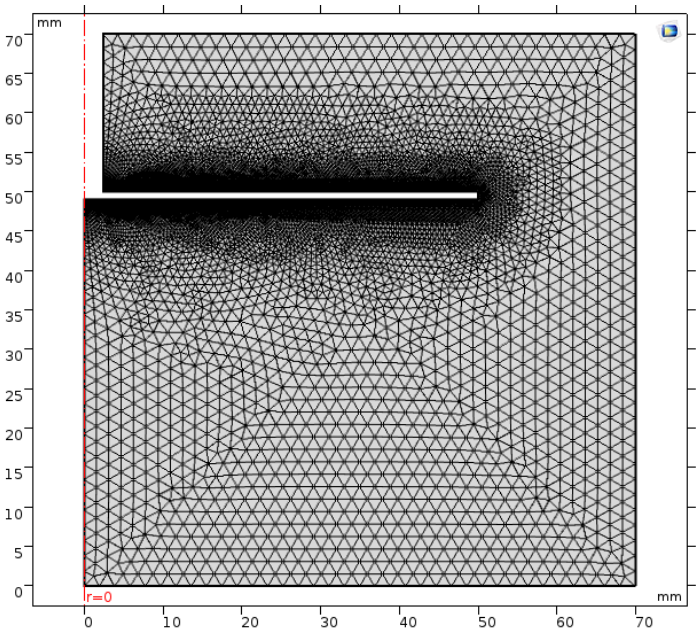

Figure 22 Initial triangular mesh in single-phase turbulent flow model using COMSOL®, for detachment study

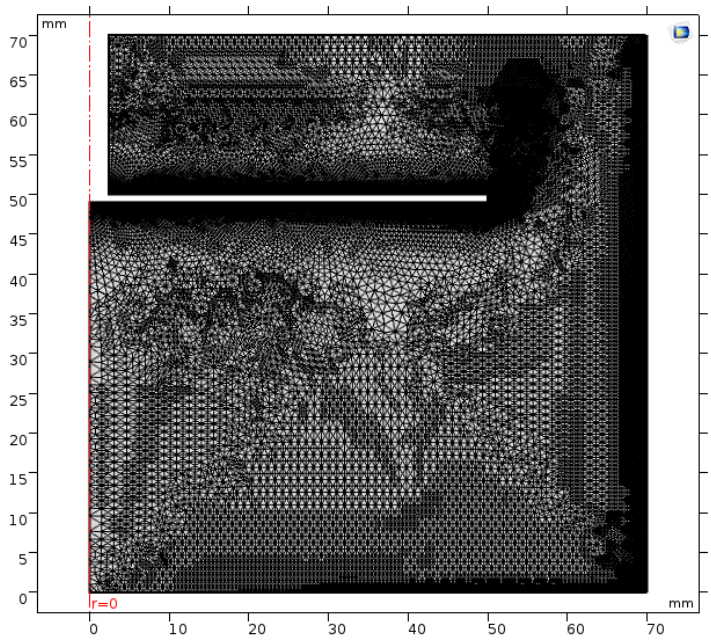

Figure 23 Final mesh after adaptive mesh refinement analysis in single-phase turbulent flow model using COMSOL®

3.2. Flow induced by a spinning disk in the presence of suspended particles

The bacterial attachment study was carried out to predict the amount of shear stress induced by the rotating of the disk, and its effect on the transfer and attachment of bacteria from contaminated water to a clean leaf.

In the benchtop device, it was assumed that a piece of clean leaf was attached to the bottom center of the rotating disk (geometry of the leaf not shown nor studied in numerical simulation). Geometry and details of the benchtop device are specified in the following section. The cylindrical tank was filled with water containing organic matter. To study bacterial transfer from the organic matter to water and the attachment of bacteria from water to the clean leaf, in the presence of suspended particles, the organic particles were inoculated with bacteria. The leaf attached was clean and no viable bacteria were initially attached on it. The final count of the leaf demonstrated the number of bacteria attached. In the experiment carried out by UC Davis team, agarose beads were used to simulate the organic matter and were inoculated with *Escherichia coli* O157:H7-*lux*. In numerical simulation, the organic particles were assumed to be uniformly suspended in the fluid.

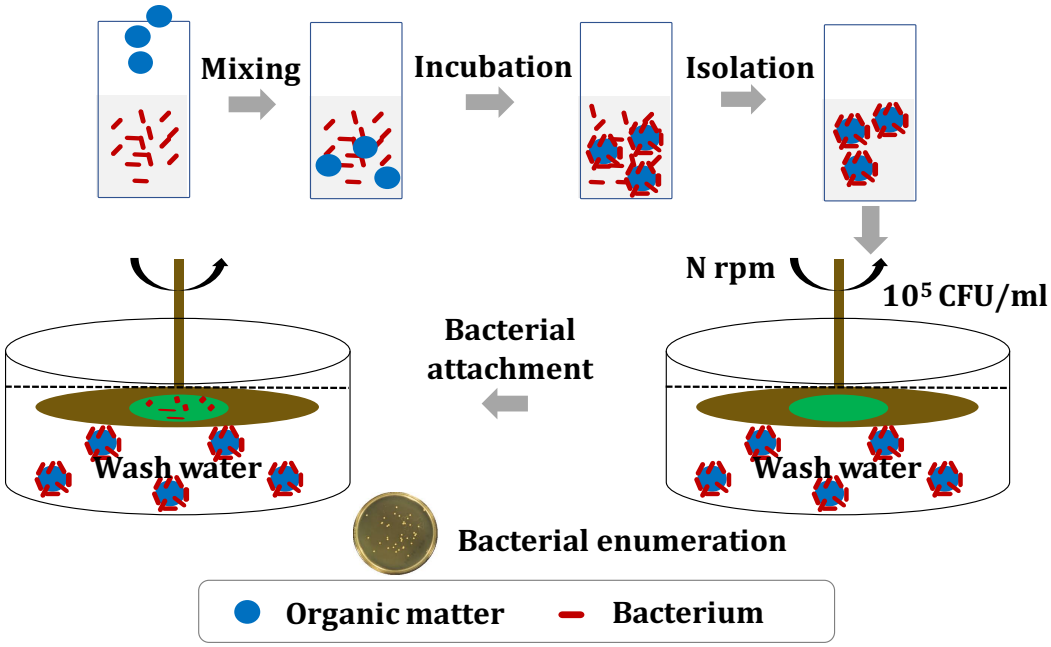

Figure 24 Diagram representing the cross-contamination experiment (at UC Davis, Dr. Nitin's group)

3.2.1. Geometry

The benchtop device used for the bacterial attachment study (experiments conducted at UC Davis, by Dr. Nitin's group) was similar to the one described in the previous section, but some changes were made. The dimensions of the device for bacterial attachment study are shown in the Fig. 25. As shown in the figure, the rotating disk was thicker compared to the previous one.

Dimensions of the geometry used in the numerical simulation were the same as those in the experimental setup which consisted of the rod, the disk and the outer cylinder. The dimensions of each part were: Height of the rod: h_r = 6 mm, radius of the rod r_r = 7 mm; thickness of the disk h_d = 14 mm, radius of the disk r_d = 50 mm; Height of the outer cylinder H_c = 60 mm, radius of the outer cylinder R_c = 70 mm.

To simulate the organic matter, spherical particles were considered. The diameter of each suspended particle was 100 μm. The volumetric density of the suspended particles was 100 (number of particles/ml), the calculated volume fraction of suspended particles was 0.005%. The pressure distribution is calculated from a mixture averaged continuity equation and the velocity of the dispersed phase is described by a slip model. The volume fraction of the dispersed phase (organic particles in our case) is tracked by solving a transport equation for the volume fraction.

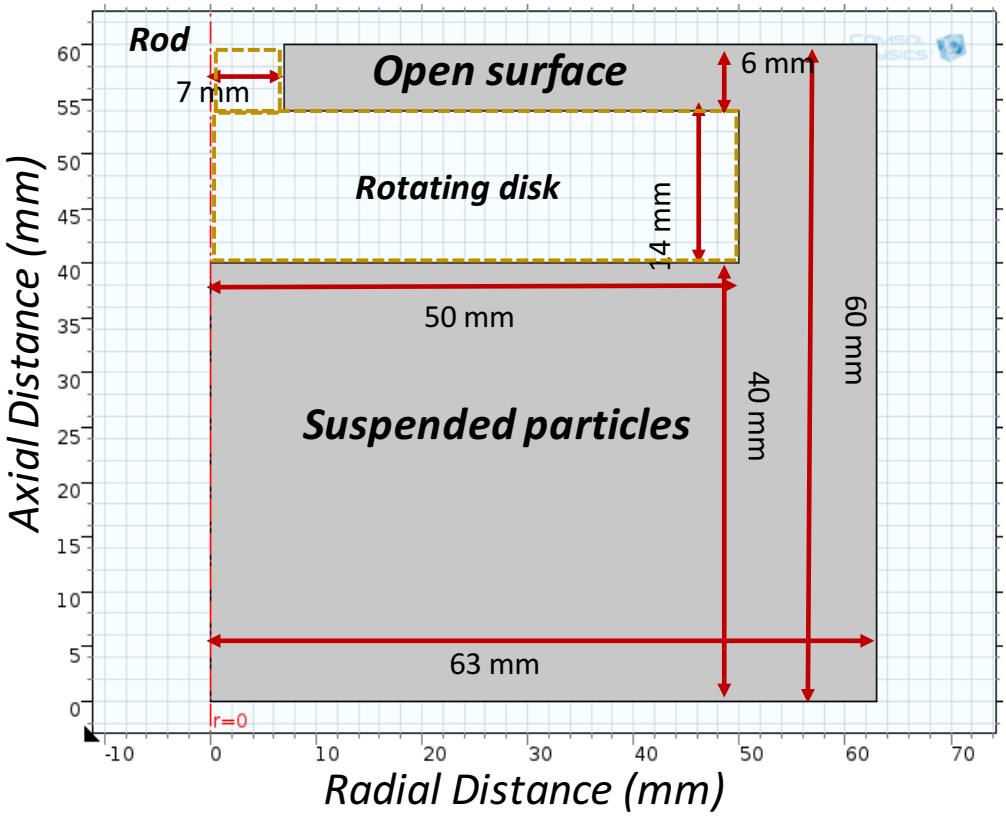

Figure 25 Dimensions of the benchtop device in k-ε turbulent flow model used for attachment study, with 0.005% suspended particles; Rod and rotating disk were marked with dotted lines

3.2.2. Boundary conditions

For numerical purposes, since the geometry was rotationally symmetric, a simplified 2D axisymmetric turbulent model was used. The 3D geometry to exemplify the actual experimental design (shown in section 2.1, Fig. 16) in COMSOL® Multiphysics is not shown here. The geometry used in numerical simulation is shown in Fig. 20, which shows a radial cross section of the whole geometry. All three velocity components exist in the flow induced by the spinning disk, swirl flow module with three velocity components [v_r – radial velocity (m/s), v_z – axial velocity (m/s), v_θ – circumferential velocity (m/s)] were used. Turbulent mixture model in COMSOL® was used since the agarose beads were suspended in water and there were two phases in the geometry: solid phase: suspended organic particles; continuous phase: flow induced by the rotating disk. In the bacterial attachment study, similar to the detachment study, simulations were carried out at rotating speeds of 100 rev/min and 200 rev/min for which the flow is in turbulent regime. Thus k-ε turbulent flow model was used to simulate the turbulent flow. The k-ε model uses wall function and is the most common model used to solve fluid dynamic problems. It has good convergence rate and relatively low memory requirements of the computer.

Boundary conditions used in the simulation included:

a. Sliding wall as the inlet boundary condition for the rod and the rotating disk, $v_r = v_z = 0$ m/s and $v_\theta = \omega r_r$ m/s, where $\omega = 2\pi N/60$ is the angular velocity (rad/s), N is the input rotating speed (rev/min);
b. No slip boundary conditions at the wall of the outer cylinder, where $v_r = v_z = v_\theta = 0$ m/s;

c. The average turbulence levels were evaluated in the flow (k, ε) along the rotating walls in the single-phase model discussed in the earlier section. In the turbulent multiphase flow model, the inlet turbulence properties were specified with "Specify turbulence variables" and then the values of turbulent dissipation rate (ε) and turbulent kinetic energy (k) calculated from the single-phase results were entered. Limitations of the methodology regarding the turbulence level at the rotating wall are discussed in the following section.

d. Initial values were zero ($v_r = v_\theta = v_z = 0$ m/s) for the continuous phase (water) in the domain. Certain number of volume fraction was set in the initial condition since it was initially in the water domain. No dispersed phase flux was applied as the dispersed phase boundary condition since the particles were initially in the continuous flow and were dispersed due to the rotation of the disk.

e. Volumetric fraction of the dispersed phase was 0.005%, as the initial condition.

f. Symmetry on top of the outer cylinder which is the free water surface;

g. Point pressure constraint feature was added and applied at one point of the geometry, since it was not possible to specify a pressure level using any boundary condition as an outlet. The gage pressure was set as zero at point 3 specified in Fig. 20**.**

h. Due to the density difference between the fluid and the particles, it is possible that the particles will sink to the bottom of the tank or buoyantly rise, therefore the gravitational force was included.

The boundary conditions used in the mixture model corresponded to the ones used in the single-phase model used for microbial detachment study mentioned in earlier section, where more detailed information can be found.

Material properties and computational mesh

Properties of water (density ρ=1000 kg/m^3, viscosity μ=0.001 Pa·s) were used for the fluid flow, particle properties were: density ρ = 1100 kg/m^3, diameter d = 100 μm. Based on the flow experiment conducted in the benchtop device (by UC Davis, Dr. Nitin's group), when the disk was rotated at 100 rev/min and 200 rev/min respectively, the flow observed was in turbulent regime. Free triangular mesh was used in the computational domain. Mesh was refined gradually till the change in solution was negligible, and relatively constant solution was achieved. Finer mesh was defined along the radius of rotating disk since this was of research interest. The final solution was mesh independent and the final mesh contained 44313 elements, as shown in Fig. 26. The relative tolerance for the convergence criterion was 10^{-6}. The total computational time required was 868 seconds and 924 seconds when the disk was rotated at 100 rev/min and 200 rev/min respectively, for an unsteady state study conducted within 2 min. The simulations were carried out on a DELL Inc. workstation with Intel® Xeon® processor with 64 GB RAM.

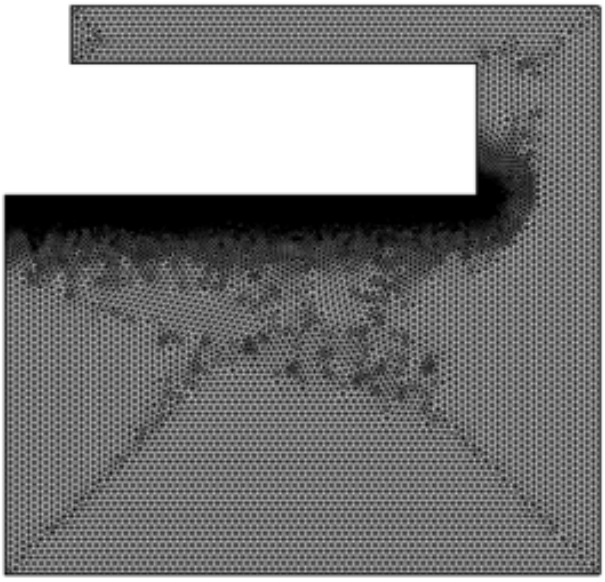

Figure 26 Final mesh used in mixture turbulent flow model (radial section of the geometry) by COMSOL® simulation.

Calculation of shear stress

There were no predefined variables for wall shear stress in the multiphase turbulent module in COMSOL®. The shear stress was defined on the wall using the viscous stress subcomponents (τ_x, τ_y, τ_z).

3.3. Ordinary differential equation (ODE)-based model for bacterial detachment and attachment in wash water in the absence of sanitizers

3.3.1. Rationale

A lot of research has been conducted to study the adhesion of cells to produce surfaces. There is adequate evidence to suggest that the cells which possess certain types of receptors are able to bind highly selectively to those complementary molecules and ligands on a targeted produce surface. This highly selective interaction between cells and

the target surface is mediated by "receptor-ligand binding", as concluded by the researchers. A mathematical model was thus proposed to describe and quantify such adhesion and detachment interaction (Wang and Bryers, 1997).

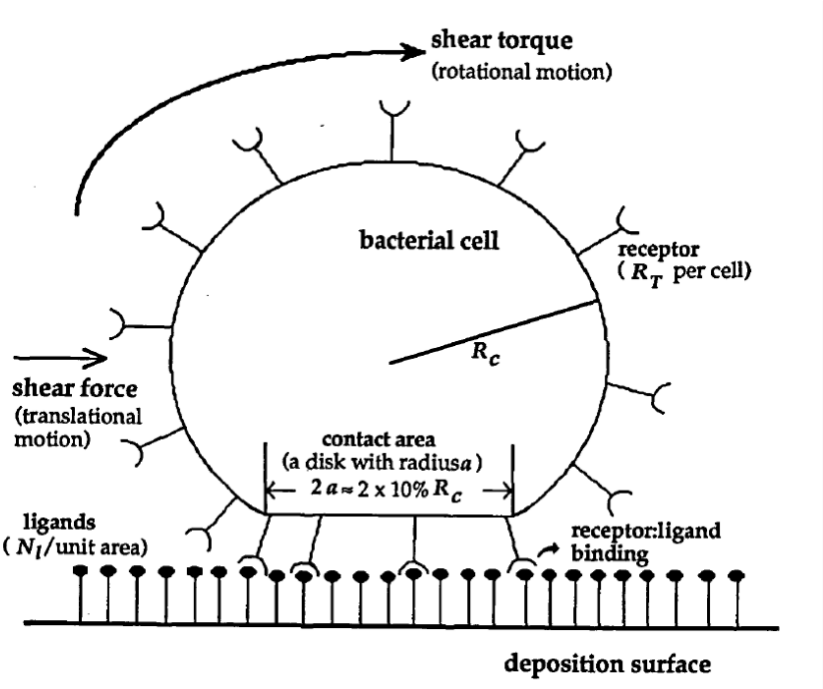

Figure 27 Schematic representation of the point-attachment model

A Schematic representation of the bacterial attachment model was shown in Fig. 27. It was assumed in the point attachment model that the bacterial cells were ideal spheres and were covered uniformly with spring-like receptors. The number of receptors in each cell is different and depends on the bacteria itself. Within the binding area of the surface, which is called the "contact area", ligands were naturally attached, and certain number of ligands would form specific bonds with the receptors. The density of ligands coated on the deposition surface is an intrinsic property of each produce and differs from type to type. Since bacteria do not spread upon attachment, it was assumed that the receptors of

cells do not move when the bacterial cells move and the contact area on the surface of produce remains constant.

This point-attachment model proposed the mechanism of bacterial adhesion and detachment as mediated by the receptor-ligand binding. In the uniform fluid flow where shear forces were induced, the shear force exerted on the bacterial cells thus renders both the translational and rotational movement of bacterial cells. Under such shear flow, when bacterial cells move into the contact area, some of the receptors of the bacterial cell would form the specific binding with ligand on the surface. It should be noted that only the receptors within the contact area will form bonds and thus mediate further adhesion. As the shear forces grew stronger and when the bacterium cell could not stand the force, the bond between the cell receptor and the ligand would break thus the bacterium cell was detached.

The equations were modified based on the dynamic model and ordinary differential equations proposed by Wang and Bryers (1997), as discussed in section 1.5. In the model system, the reactor was where the attachment and detachment took place. In our benchtop scale washer system, the reactor was a cylindrical water tank. As shown in the Schematic Fig. 28, fluid flow of certain volumetric flow rate Q (ml/min) carrying bacteria of initial load X_{in} (cells/ml) came into the reactor, and the flow kept coming in and out through the reactor tank. Certain number of bacteria were attached to the target surface mediated by attachment rate R_1. The bacteria attached to the targeted leaf surface were mediated by the receptor-ligand binding, and some of the bacteria loosely attached were detached when the receptor-ligand binding broke. Detachment of bacteria was controlled by the detachment rate denoted as R_2 in the Fig. 28.

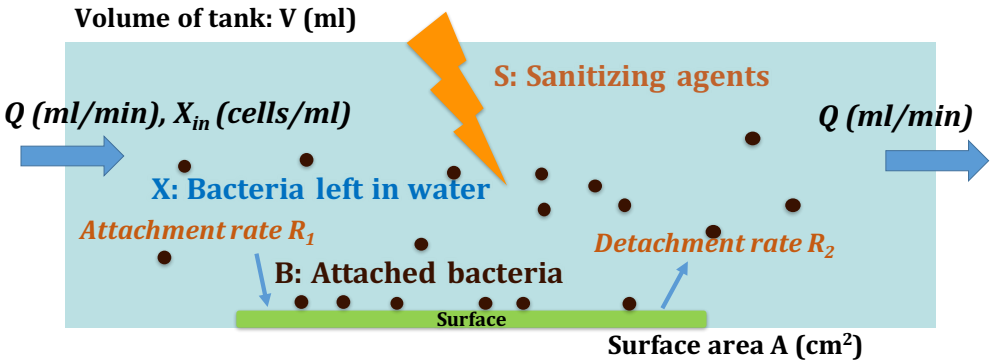

Figure 28 Schematic diagram of the microbial attachment and detachment in the presence of sanitizer agents under shear flow

Equations to quantify the attachment and detachment of bacteria in water system were derived on the basis of mass transfer. The volume flow rate of fluid flow was kept constant during the process.

a. Governing equation:

$$Q_{in} = Q_{out}$$

.....(3.9)

where Q_{in} is the volumetric flow rate of flow entering the tank (ml/min) containing X_{in}; Q_{out} is the volumetric flow rate of flow leaving the tank (ml/min) containing X.

b. For bacteria suspended in water: the change of bacteria suspended in water with time is a function of bacteria carried by flow into the tank, minus the bacteria carried by flow out from the tank, minus by the number of bacteria attached to the surface from water, plus the number of bacteria detached from leaf surface to wash water.

$$\frac{d[XV]}{dt} = X_{in}Q - XQ - R_1 + R_2$$

.....(3.10)

$$\frac{dX}{dt} = \frac{Q}{V}[X_{in} - X] - \frac{R_1}{V} + \frac{R_2}{V}$$

.....(3.11)

in equation (3.10) and (3.11), the attachment rate R_1 was defined as:

$$R_1(^{cell}/_{s}) = K_{adh}(^{cm}/_{s})A(cm^2)X(^{cell}/_{cm^3})$$

.....(3.12)

where K_{adh} was the attachment rate constant and the values were given out by Wang and Bryers, (1997). The rate of attachment from wash water to the target leaf surface was a function of the total bacteria suspended in water, the area of surface, and was mediated by attachment rate constant K_{adh}. A was the substratum reactor surface, V was the volume of reactor. The values of Q, A and V were obtained from Hammer and Lauffenburger (1987).

The detachment rate R_2 was defined as:

$$R_2(^{cell}/_{s}) = B(^{cell}/_{cm^2})A(cm^2)k_{det}(^{1}/_{s})$$

.....(3.13)

where k_{det} was the detachment rate constant. According to Hammer and Laufferburger (1987), k_{det} was found to be a function of shear stress that exerted on the leaf. Further discussions about the effect of the value of k_{det} on the detachment rate, and on cross-contamination of bacteria in water are in section 4.4.

Thus, equation for suspended bacteria in water was defined as:

$$\frac{dX}{dt} = \frac{Q}{V}[X_{in} - X] - K_{adh}\frac{A}{V}X + k_{det}\frac{A}{V}B$$

.....(3.14)

c. For bacteria attached to the leaf surface: the bacteria attached to the target surface with regards to time was mediated by the rate of bacteria attached, and the rate of bacteria detached from the surface.

$$\frac{d[BA]}{dt} = R_1 - R_2$$

.....(3.15)

$$\frac{dB}{dt} = \frac{K_{adh}AX}{A} - \frac{BAk_{det}}{A}$$

.....(3.16)

Thus, equation for attached bacteria on leaf surface was defined as:

$$\frac{dB}{dt} = K_{adh}X - k_{det}B$$

.....(3.17)

Equations (3.14) and (3.17) were solved analytically and numerically by 4th order Runge-Kutta methods and ode45 solver in MATLAB®. The results are shown and discussed in section 4.4.

3.3.2. Effect of detachment rate constant

As discussed in the earlier section, it was found by Wang and Bryers (1997) that the detachment rate constant was a function of shear stress. In this study, the effect of detachment rate constant was studied (Wang and Bryers, 1997). The equations explained above were solved both numerically and analytically. Results are shown and discussed in section 4.4.

3.3.3. Values of parameters used in the ODE model

To solve the ODE equations described above we used parameters given by Hammer and Lauffenburger (1987). In the equation (14), for X (bacteria left in water), the dilution rate which is the ratio of volumetric flow rate divided by the reactor volume, was 4 h^{-1} by (Hammer and Lauffenburger, 1987). The ratio of A/V was 10 cm^{-1}. Attachment rate constant K_{adh} was 0.01 cm/min, base value for detachment rate constant k_{det} was 0.007 min^{-1}. To study the effect of k_{det}, two other values were chosen: one 10 times smaller than the base value: 0.0007 min^{-1}, and one 10 times higher than the base value: 0.07 min^{-1}. The values used here were for research purposes only.

3.4. Ordinary differential equations for bacteria detachment and attachment study in the presence of sanitizers in wash water

In the previous section, ordinary differential equations were derived based on mass balance, describing the cross-contamination behavior (attachment of bacteria from water to produce surface, and detachment of bacteria from attached surface to flowing water) without the addition of sanitizers in wash water. The previous case was only valid when no organic load was generated during processing.

As discussed in section. 1, sanitizers are used in commercial fresh produce processing systems, coupled with washing by mechanical forces. Organic matter such as soil and debris are carried by flowing fluid and are continuously generated during produce washing. In this section, the use of sanitizer in a produce washing system is considered. The addition of sanitizer resulted in the changes of the concentration of suspended bacteria in water. It is worth noting that the sanitizers are more effective in inactivating

microbes in wash water, compared to those on the produce surface (Gil et al., 2009). In our ODE system, the change in the concentration of attached bacteria was reflected by the change of suspended bacteria. The direct influence of sanitizer on the attachment of bacteria was not considered here.

The parameters used in the ODE system were obtained by carrying out experiments in pilot plant scale washer system from (Luo et al., 2012). Our ordinary differential equations were developed so as to apply them to commercial processing conditions. Therefore, the data from (Luo et al., 2012) and (Munther et al., 2015) were considered adequate to be used in our case. Detailed information was given in introduction section.

3.4.1. Rationale

Three variables were included in the improved ODE system: the suspended bacteria in water (X: cells/ml), the attached bacteria on produce surface (B: cells/ cm^2), and chlorine sanitizer (S: mg/L).

a. Governing equation: $Q_{in} = Q_{out}$, where Q_{in} is the volumetric flow rate of flow initially entering the tank (ml/min); Q_{out} is the volumetric flow rate of flow leaving the tank (ml/min).
b. For the chlorine sanitizer (S: mg/L) used: the depletion of sanitizer resulted in three ways: The sanitizer was used for the inactivation of microbes in water; the depletion of sanitizer due to the organic matters in water, chemical and biological oxygen demand generated with time during reaction; and finally, the natural decay of chemical sanitizer. Thus, the equation describing the concentration of sanitizer consisted of the addition of sanitizer by the continuous fluid flow entering the reactor

tank, and flow continuously leaving the reactor tank, the depletion of chlorine sanitizer by reacting with organic loads and the natural decay with the change of time.

The change of **chlorine (S)** was given by the following equation:

$$\frac{dS}{dt} = D(S_{in} - S) - \lambda_c S - \beta_c OS$$

.....(3.18)

where S_{in} is the concentration of chlorine initially entering the produce washing tank; S denotes the concentration of chlorine in the washer tank and is also the concentration of chlorine in the outgoing flow; λ_c is the natural decay rate constant of free chlorine, the value of the rate constant was obtained from (Hua et al., 1999); β_c is the depletion rate of free chlorine in wash water, the value of the parameter was obtained from experiments conducted by (Luo et al., 2012); O (mg/L) is the chemical oxygen demand in wash water. The rate of increase of chemical oxygen demand was modeled as:

$$\frac{dO}{dt} = k_0$$

.....(3.19)

where k_0 is the constant of increased chemical oxygen demand in industrial scale washing system (Munther et al., 2015).

c. For bacteria suspended in water (X: cells/ml): The bacteria in the fluid flow were mediated by detachment and attachment rate constant, as defined and explained in the previous section. Also, the number of free bacteria suspended in the flowing fluid decreased due to the inactivation by free chlorine.

The rate of change of **suspended bacteria (X)** was defined as:

$$\frac{dX}{dt} = D(X_{in} - X) - K_{adh}X\frac{A}{V} + k_{det}B\frac{A}{V} - \alpha XS$$

.....(3.20)

where α is the inactivation rate of pathogens by free chlorine (L/(mg·min)). The change of suspended bacteria was mediated by the detachment rate constant and the amount of sanitizer left in wash water, results and discussions are demonstrated and discussed further in the following section.

d. For bacteria attached to the produce surface (B: cells/cm^2): In the presence of chlorine (sanitizer), the bacteria attached to the surface were dominantly mediated by the change of number of suspended bacteria in wash water.

The rate of change of **bacteria attached (B)** was defined as:

$$\frac{dB}{dt} = K_{adh}X - k_{det}B$$

.....(3.21)

K_{adh} is the attachment constant rate, k_{det} is the detachment constant rate. Equations (3.18), (3.19), (3.20) and (3.21) were solved numerically by MATLAB®.

3.4.2. Values of parameters used in the ODE model

Besides the parameters used in the previous ODEs described in section 2.3.3, additional terms and parameters were taken from Munther et al. (2015) & Luo et al. (2012). Values used are shown in the table below:

Table 2 Values of parameters used in ODE model by (Munther et al., 2015 & Luo et al., 2012)

Source	Parameters	Description	Values & units
From (Luo et al., 2012)	k_0	COD increase rate in the pilot plant scale produce washer	32.3 mg/(L∗min)
Calculated from (Huang et al., 1999)	λ_c	Natural decay rate of free chlorine	1.7×10^{-3} 1/min
Model fit by (Munther et al., 2015)	β_c	Depletion rate of free chlorine in wash water	5.38×10^{-4} L/(mg∗min)
	α	Inactivation rate of pathogen via free chlorine	0.75 L/(mg∗min)

4. RESULTS AND DISCUSSIONS

First, the flow induced by a rotating disk in an infinite medium was simulated. The numerically predicted results were compared with theoretical results to validate the methodology used for detachment and attachment studies. Once the methodology was validated, the numerical simulation was conducted for the benchtop scale device in the absence of suspended particles and in the presence of particles, respectively. The flow fields with total velocity vectors were plotted to visualize the flow induced at two different rotating speeds: 100 rev/min and 200 rev/min. Shear stress values along the radius of the leaf attached to the bottom of the rotating disk were predicted using numerical simulation. The values of shear stress generated without and with suspended particles in the fluid were predicted and compared between actual microbial detachment and attachment studies conducted at UC Davis by Dr. Nitin's group. In another approach, using a different mathematical model, the number of microbes detached, transferred and attached from flowing water to produce surface as affected by the shear stress was quantified using ordinary differential equations.

4.1. Numerical results of turbulent flow in single-phase model

This section includes the validation of methodology used for boundary conditions, and the results from single phase model without suspended particles.

4.1.1. Numerical results of flow in an infinite medium

A comparison of shear computed by COMSOL®, with analytical results is shown in Fig. 29, which also shows the theoretical results on the same graph. In Fig. 29, total shear stress along the radius r_d was numerically calculated and is shown in red. The details of

the theoretical results are described in the next section, and the comparison of numerical results with theoretical (analytical) results are also discussed.

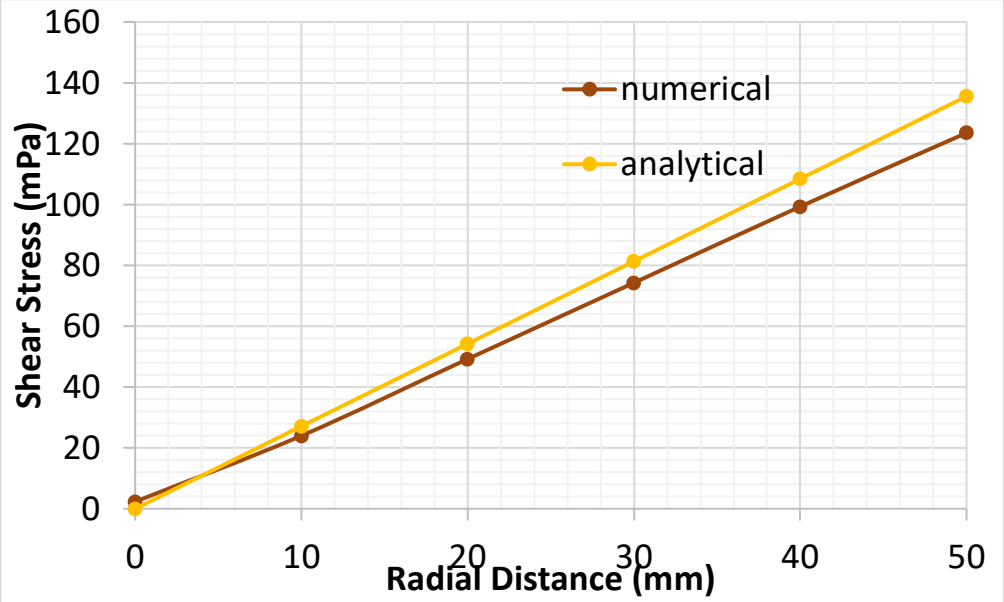

Figure 29 Comparison of numerical and analytical results for flow induced by a disk rotating in a fluid at rest (Schlichting, 1979)

Comparison with theoretical results

In an infinite medium where the fluid flow was at rest initially, when a disk is rotated at constant angular velocity ω, the shear stress (τ, Pa) on the disk surface due to the induced laminar flow can be calculated as (Schlichting, 1979):

$$\tau = 0.792\rho r\nu^{1/2}\omega^{3/2}$$

.....(4.1)

in equation (4.1), ρ is density (kg/m^3), r is radial distance (m), ν is kinematic viscosity (m^2/s) and ω is the angular velocity (rad/s).

As shown in Fig. 29, the shear stress induced at the edge of disk was slightly lower than the value calculated theoretically. The difference is not significant and may due to

the boundary in the numerical simulation, i.e., numerical simulation cannot be carried out in an infinite domain. Overall, the numerical results corresponded reasonably well with analytical results and the boundary conditions used for the rotation of disk in subsequent numerical simulations were thus validated.

4.1.2. Flow profile and total velocity vectors of flow in single-phase model in benchtop device

The flow profile was plotted using COMSOL® Multiphysics in 2D axisymmetric turbulent single-phase model. As described earlier in section 3.1, the numerical simulation was conducted in the radial cross section and the results obtained in this section were replicated for the rest of the geometry. As shown in Figs. 30 & 31, different velocity magnitudes were shown in lighter to darker color shades. In Fig. 30, when the disk was rotated at 100 rev/min, the edge of the rotating plate showed the highest value of velocity of 0.15 m/s to 0.25 m/s. Arrows in the figure show the total velocity vectors. In the area above the rotating plate, the flow stirred by the rotation of disk had higher velocity above the disk partially due to the free surface at top of the tank, which offered no resistance to flow. In the region below rotating plate, higher velocity was observed close to where the leaf was attached: the bottom center surface of the plate. Theoretically, higher the velocity near surface should result in higher the shear stress. In the region above the disk where higher velocities take place, circular motion can be seen due to the imposed tangential velocity of the plate. Results showed similar pattern when the disk was rotated at 200 rev/min, as seen in Fig. 31. From flow field, shear stress values were

calculated along the radius of leaf attached to the bottom of the disk. Results of shear stress calculation and further discussions are given in the following section.

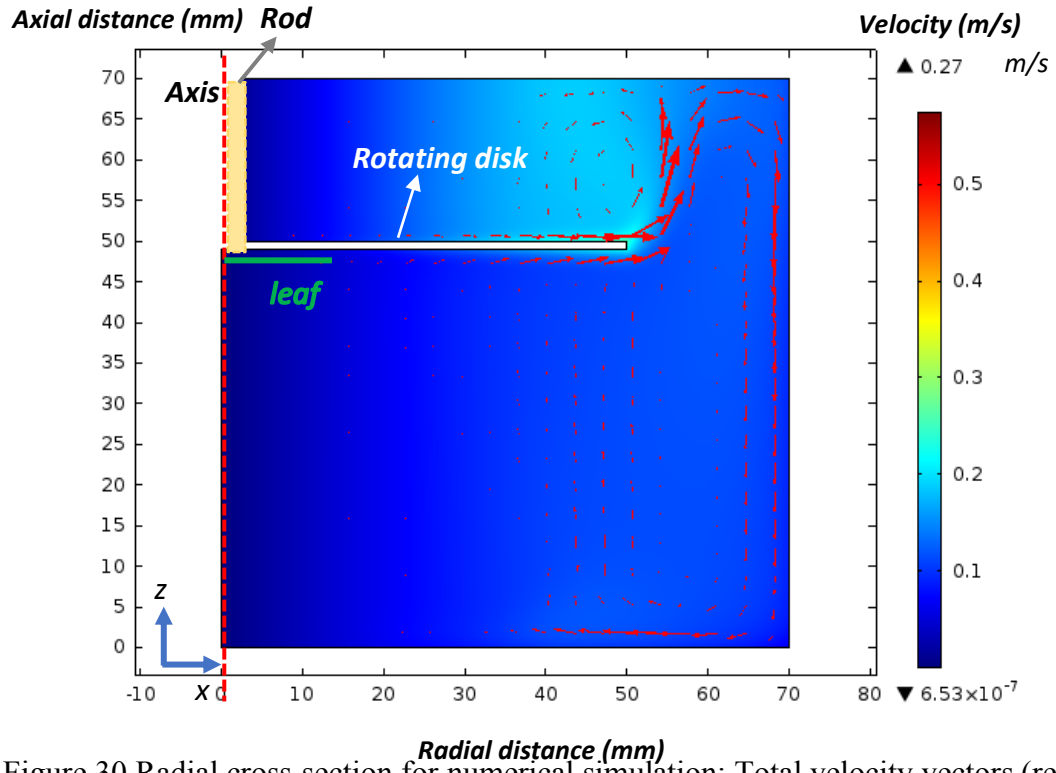

Figure 30 Radial cross-section for numerical simulation: Total velocity vectors (red arrows) when the disk rotated at N = 100 rev/min, angular velocity ω = 10.47 rad/s, in the turbulent flow field without suspended particles. Axis: Red dotted central line; Central rod: yellow cylinder; Rotating disk: white cylinder; Attached leaf: green line.

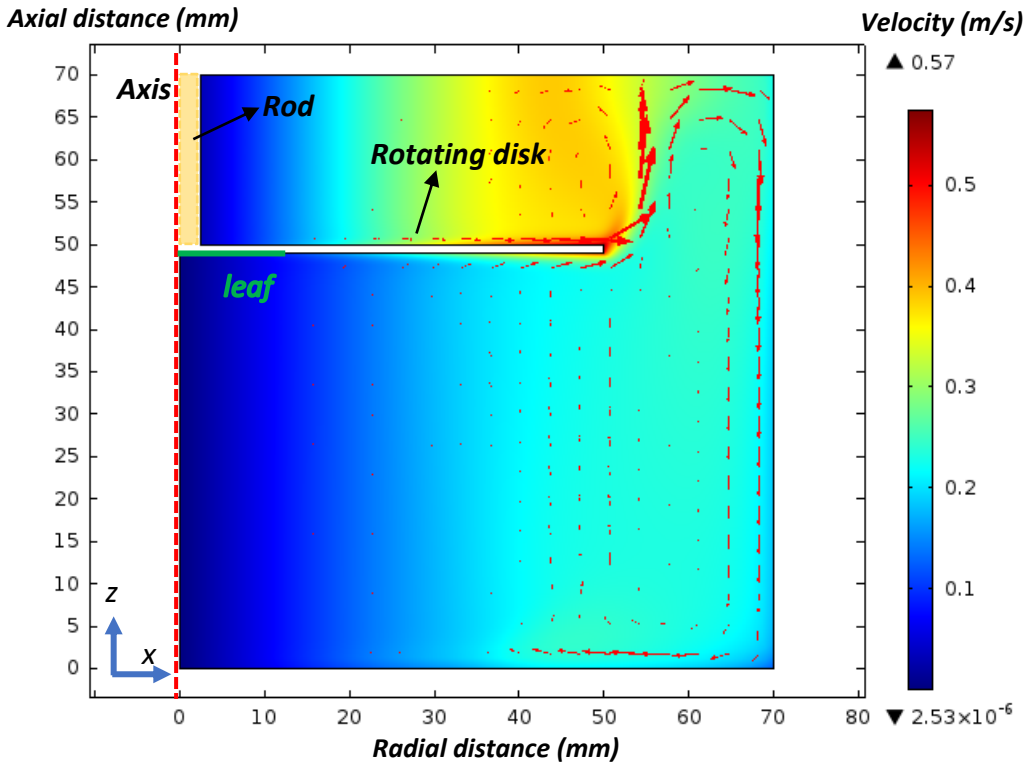

Figure 31 Radial cross-section for numerical simulation: Total velocity vectors (red arrows) when the disk rotated at N = 200 rev/min, angular velocity ω = 20.94 rad/s, in the turbulent flow field without suspended particles. Axis: Red dotted central line; Central rod: yellow cylinder; Rotating disk: white cylinder; Attached leaf: green line.

4.1.3. Shear stress values on the leaf surface in the absence of suspended particles

The shear stress on the bottom of the rotating disk was obtained using the COMSOL® 2D axisymmetric swirl flow model as described in section 3.1. Shear stress was calculated using the built-in wall shear stress feature in COMSOL®. Calculated shear stress values are plotted on the y-axis against radial distance on the x-axis for two different rotating speeds 100 rev/min and 200 rev/min. The plot of shear stress on the leaf surface as a function of radial distance is shown in Fig. 32. The radial distance varied

from 0 mm to 15 mm, as the radius of leaf attached was 15 mm. It should be noted that the shear stress was calculated along the entire radius of rotating disk, only the first 15 mm from the center of bottom plate were of interest.

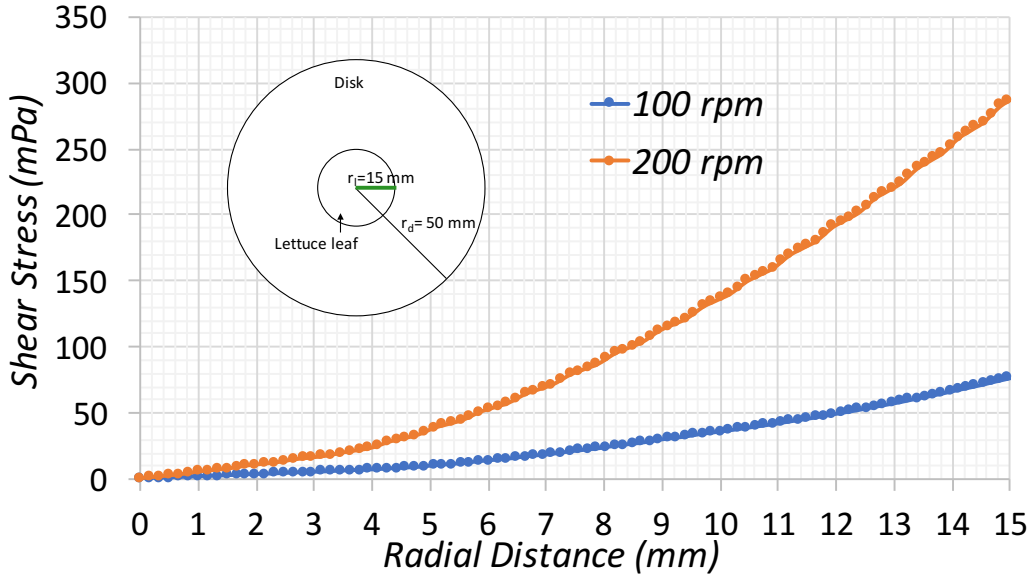

Figure 32 Shear stress along the radius of leaf calculated without suspended particles in the fluid (water)

As seen in the Fig. 32, the values of calculated total shear stress on the surface of the leaf varied from 0 mPa to 79 mPa at 100 rev/min, and from 0 mPa to 290 mPa at 200 rev/min. At the center of the attached leaf, the shear stress is zero. The value of shear stress increased gradually as the radial distance increased, because the induced flow velocity increased along the radius.

4.2. Numerical results of turbulent flow in two-phase model

4.2.1. Flow profile and total velocity vectors of flow in two-phase model in benchtop device

Figure 33 and Fig. 34 show the flow profile with velocity vectors when the disk was rotated at 100 rev/min and 200 rev/min, respectively; different colors represent different flow velocities. As shown in Fig. 33 and Fig. 34, higher velocity appears at the edge of the disk, above the rotating disk and immediately below the plate. In the presence of particles, the flow patterns were similar to those in the absence of particles. It was because of the turbulent flow induced by high rotating speed and the relatively low density of particles dispersed (diameter 100 μm, 100 particles/ml). Details have been discussed in section 4.1.2. The physical thickness of the attached leaf was not considered in the numerical simulation. The shear stress values were evaluated using the viscous shear tensors in COMSOL® and are further discussed in the next section.

N = 100 rev/min

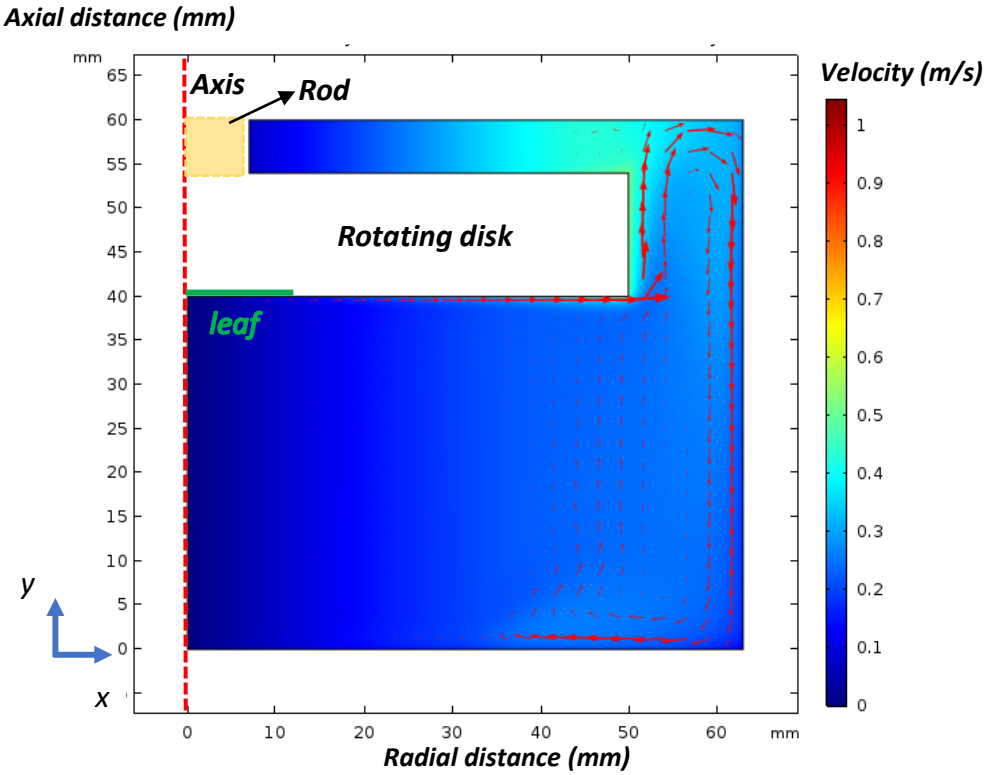

Figure 33 Radial cross-section for numerical simulation: Total velocity vectors (red arrows) when the disk rotated at N = 100 rev/min, angular velocity ω = 10.47 rad/s, in the turbulent flow field with suspended particles. Axis: Red dotted central line; Central rod: yellow cylinder; Rotating disk: white cylinder; Attached leaf: green line.

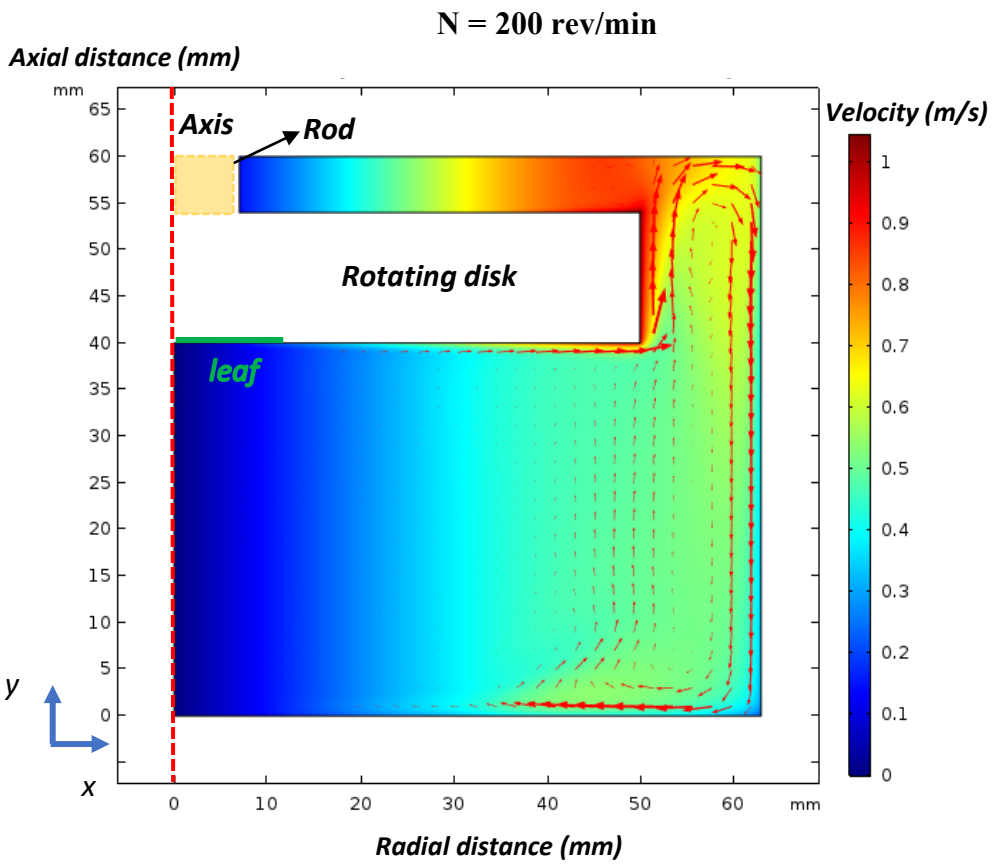

Figure 34 Radial cross-section for numerical simulation: Total velocity vectors (red arrows) when the disk rotated at N = 200 rev/min, angular velocity ω = 20.94 rad/s, in the turbulent flow field with suspended particles. Axis: Red dotted central line; Central rod: yellow cylinder; Rotating disk: white cylinder; Attached leaf: green line.

4.2.2. Shear stress values on the leaf surface in the presence of suspended particles

The shear stress values at the bottom of the rotating disk were calculated using shear tensors in the COMSOL® 2D axisymmetric swirl flow module described in section 3.2. In experiments done by Dr. Nitin's group at UC Davis, the leaves were cut in circular shape with the radius of 15mm. Shear stress was plotted as a function of the radial distance of the leaf., the plot was shown in Fig. 35. The calculated shear stress values

were from 0 mPa – 340 mPa at 100 rev/min, and the shear stress varied from 0 mPa – 987 mPa at 200 rev/min. The calculated arithmetic average shear stress values were varied between 137 mPa and 403 mPa, when the disk rotating speed was varied between 100 rev/min and 200 rev/min (The area average shear stress calculated were in the range of 69 mPa to 202 mPa, details not shown here).

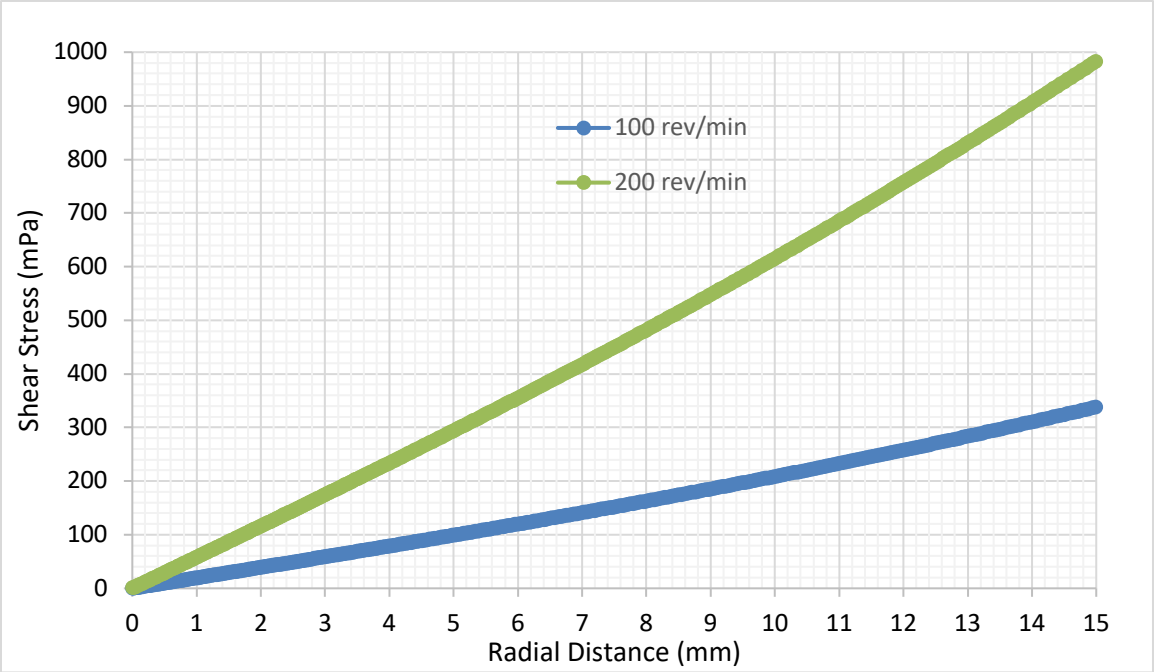

Figure 35 Shear stress calculated along the radius of leaf (0 mm – 15 mm) with suspended particles (volume fraction of 0.005%) in turbulent flow field when the disk was rotated at 100 rev/min and 200 rev/min. (The results were computed numerically in COMSOL®)

4.2.3. Comparisons of numerical predictions with/without particles in the flow

In Fig. 36 and Fig. 37, the shear stress induced in the absence of suspended particles, and in the presence of particles were compared. At rotating speed 100 rev/min, the shear stress varied from 0 mPa to 218 mPa without particles, but it varied from 0 mPa to 340 mPa with particles. Similar increase in the shear stress value was observed at rotating speed of 200 rev/min when suspended particles were added. In the corresponding experimental studies done at UC Davis, where no particles were suspended in water, the transfer and removal of bacteria from inoculated leaf surface was due to the shear force (no chemical treatment was added). While with particles in water, the computed shear stress significantly increased as according to numerical simulation. Transfer and attachment of bacteria to the leaf surface were partially due to the shear force and the contact with produce leaf surface.

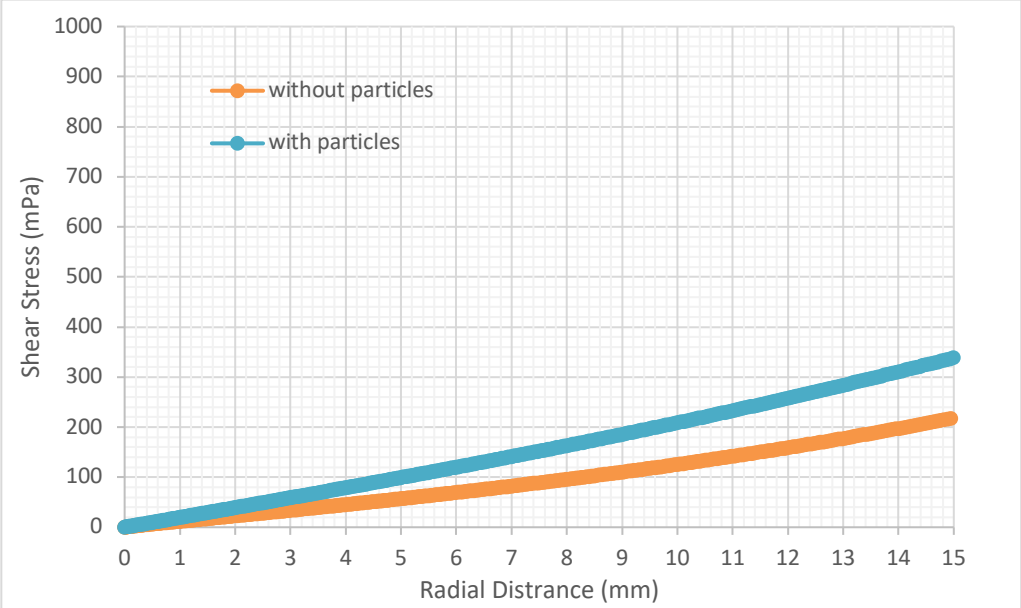

Figure 36 Comparison of numerically calculated shear stress along the radius of leaf (0 mm – 15 mm) without particles and with particles (0.005%) in turbulent flow field when the disk was rotated at 100 rev/min, in the benchtop device as shown in Fig. 27 (The results were numerically computed in COMSOL®)

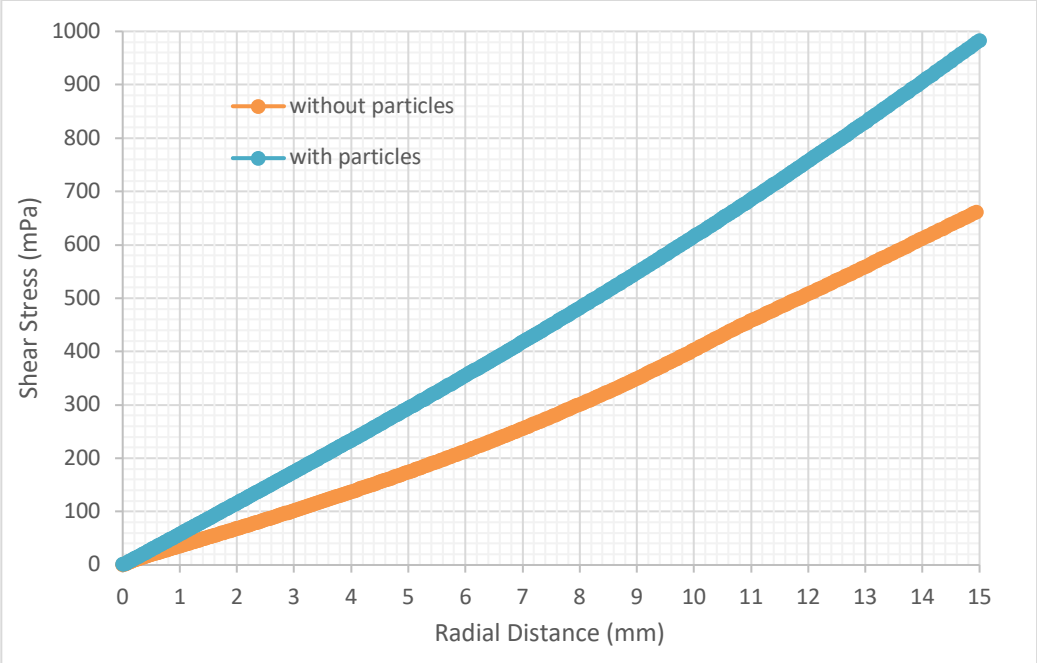

Figure 37 Comparison of numerically calculated shear stress along the radius of leaf (0 mm – 15 mm) without particles and with particles (0.005%) in turbulent flow field when the disk was rotated at 200 rev/min, in the benchtop device as shown in Fig. 27 (The results were numerically computed in COMSOL®)

4.3. Comparison of numerical predictions with experimental results

The benchtop device (at UC Davis, Dr. Nitin's group) described earlier was used in lab scale experiments to simulate the industrial scale processing conditions in industry. Numerical simulation was carried out in COMSOL® to visualize the flow profile and velocity vectors in the flow. Also, shear stress on the leaf surface was calculated to further study the effect of shear stress on the removal of *E. coli* O157:H7-*lux* (used in experiments done by UC Davis, Dr. Nitin's group) from the leaf surface under disk rotation. Experimentally, the removal of bacteria was quantified by the enumeration of

bacterial population and measured by bioluminescence intensity and validated by bioluminescence imaging (done by Dr. Nitin's group at UC Davis).

Table 3 Numerically calculated shear stress when the disk was rotated at 100 rev/min and 200 rev/min; and experimentally measured (UC Davis) corresponding microbial reduction under shear

Rotating Speed		N = 100 rpm	N = 200 rpm
Detachment Study	Shear stress range	0 mPa – 79 mPa	0 mPa – 290 mPa
	Microbial reduction	1 log CFU/cm^2 reduction	1.5 log CFU/cm^2 reduction
Attachment Study	Shear stress range	0 mPa – 340 mPa	0 mPa – 987 mPa
	Microbial reduction	Up to 0.4% bacteria was transferred to leaf surface	

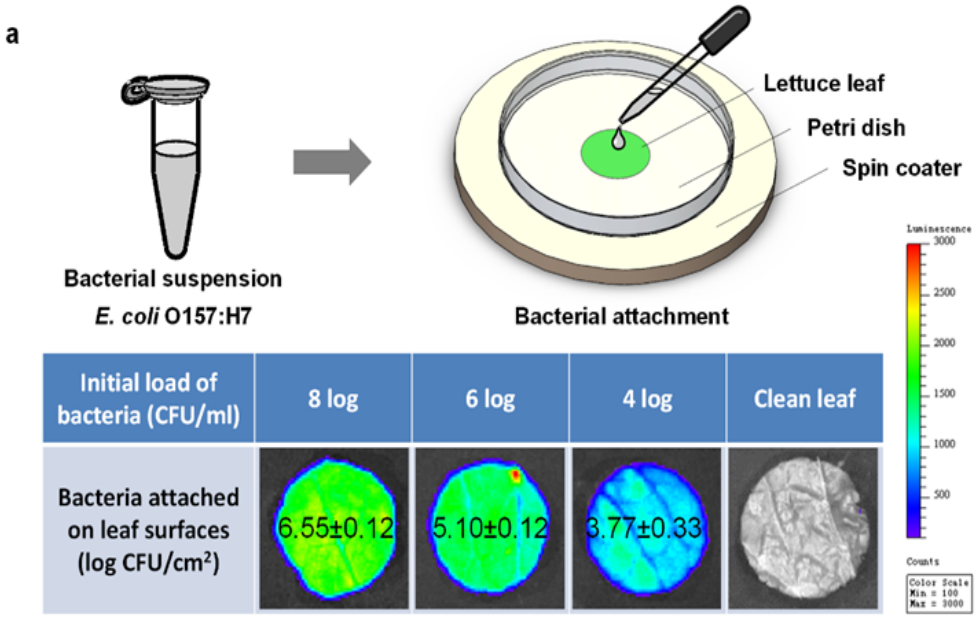

Figure 38 Bioluminescence intensity measurement (results obtained by Dr. Kang Huang at UC Davis)

4.3.1. In the absence of suspended particles in water

The number of bacteria detached from produce surface and the rate of bacteria detachment are dependent on many factors, including sanitizers and surfactants in wash water (Gil et al., 2009), washing time, and the intensity of washing, i.e., shear stress. In this study, however, only the effect of shear stress was studied using a benchtop device containing a rotating disk. As discussed in section 4.1.3, in the numerical simulation, the shear stress was calculated at two different rotating speeds 100 rev/min and 200 rev/min. In the experiments, the same conditions were used (Huang et al., 2017). The efficacy of shear-induced bacterial removal was evaluated by bacterial plate count and bioluminescence intensity measurement on leaf surface experimentally, after 20 min of rotation in the washer device. In the experiments conducted by our collaborators at UC Davis, the leaf samples were initially inoculated with *E. coli* O157:H7-*lux*. The initial microbial load ranged from 8 log CFU/ml to 4 log CFU/ml, as shown in Fig. 38. The reduction of bacterial load is shown in Table 3. At 0 rev/min, i.e., no rotation, the leaf samples were merely soaked in wash water for 20 min with no shear stress generated. No significant reduction of bacteria was observed or measured within this incubation time. Thus, it was indicated that the reduction of bacteria resulted from shear stress was independent of initial bacterial load of leaf surface. When the disk was rotated at 100 rev/min for 20 min, approximately 1 log CFU/cm^2 reduction in bacterial load was achieved. When the disk was rotated at 200 rev/min for 20 min, approximately 1.5 log CFU/cm^2 reduction was achieved due to shear stress.

The shear stress range calculated numerically for the same conditions as in the experiments, was from 0 mPa – 79 mPa at 100 rev/min, and the shear stress value varied

from 0 mPa – 290 mPa at 200 rev/min. As seen in Table. 3, with limited shear stress value, certain amount of bacterial reduction can be achieved, compared to the results of bacterial removal under static no spinning condition (when there is no shear induced, at 0 rev/min). It was observed that a small increase in the shear stress resulted in significant difference in the detachment of bacteria from leaf surface. The range of shear stress generated by the rotating disk system was adequate to induce significant detachment of bacteria. Previous literature has reported that shear stress values were in the range of 20 mPa – 2400 mPa in micro-fabricated leaf surface in the attachment study of *E. Coli* O137:H41 (Sirinutsomboon and Delwiche, 2013). It should be noted that the shear stress values in our study were calculated without considering the roughness of lettuce leaf surface, which might have resulted in a lower calculated value compared to the actual shear exerted on bacteria.

To conclude, shear force is necessary for removal of bacteria from produce surface. It can be indicated that under commercial processing conditions, the removal of bacteria can be enhanced by increasing the shear stress. In this study, only the effect of shear stress was considered and other factors such as the effect of washing time, the roughness of leaf surface was not taken into account. The results are in agreement with prior research that have suggested shear-induced detachment of bacterial from diverse biological surfaces (Warning and Datta, 2013).

4.3.2. In the presence of suspended particles in water

Experimental results showed that some (up to 0.4%) bacteria were transferred from organic loads (experimentally, agarose beads were used) to the leaf surface in the

presence of shear force, suggesting that the transfer and the attachment can take place in the presence of shear stress. Also, it was noted that in the presence of suspended particles, shear stress increased which might have resulted in more detachment of bacteria from organic load and the transfer back to water.

In the mixture model where the organic particles were assumed uniformly suspended in water, the turbulence levels should correspond to what is generated by the rotating wall. However, since the predictions of turbulence levels with benchmark calculation was difficult in this case, the turbulence levels (kinetic energy k and turbulent dissipation rate ε) were evaluated in the single-phase model previously created in bacterial detachment study. The turbulence levels calculated from single-phase model results were thus used as input for the mixture model. The shear stress on the wall was calculated using off-diagonal components of the viscous stress tensor. It should be noted that the turbulence conditions at the rotating wall were likely to be different in the case with suspended particulates versus the single-phase flow simulation. Using the turbulence levels evaluated from single-phase flow simulation at the rotating wall in the two-phase model simulation probably does not accurately represent what physically occurs, i.e., the effect of particulates on the flow was neglected on the wall. Perhaps the mixture two-phase model could be further modified and improved using other numerical software.

4.4. ODE model results without sanitizers in water

In this section, ordinary differential equations were developed and used to quantify the bacterial detachment from produce surface to fluid flow. The ordinary differential equations proposed here described the ideal case wherein no sanitizers were added into

the fluid at this stage. The cross-contamination of bacteria in the flowing fluid under this case was mediated by shear force only. The set of two differential equations was solved at three different detachment rate constants k_{det} which are influenced by shear force induced by flowing fluid. Further, the cross-contamination behavior with sanitizers added in the flowing fluid was studied and described in section 4.5.

4.4.1. Prediction of bacterial detachment and attachment without sanitizers in water as a function of time

The rate of bacteria suspended in water was denoted as X, and the rate of bacteria attached to the produce surface was denoted as B. The detachment rate constant k_{det} was set as input, and the three values for k_{det} chosen were 0.007 min^{-1} (base value from (Wang et al., 1997)), 0.0007 min^{-1} and 0.07 min^{-1}.

Equation (14) and (17) in section 3.2.1. were solved numerically. A MATLAB®code was developed as shown in Fig. 39.

```
function [t,x] = f(k)
t = 0:0.01:120;

xinit = [0,0];

    function dxdt = rhs(t, x)
        dxdt = zeros(size(x));
        dxdt(1) = (2/30)*(10^6 - x(1)) - 0.01*10*x(1) + 10*k*x(2);
        dxdt(2) = 0.01*x(1) - k*x(2);
    end

[t, x] = ode45(@rhs, t, xinit);

end
```

```
figure
for k=[0.0007, 0.007, 0.07]
[t, x] = f(k);
semilogy(t, x(:,1));
hold on;
end
xlabel('t (min)');
ylabel('X (cells/ml)');
legend('k = 0.0007 min^{-1}','k = 0.007 min^{-1}','k = 0.07 min^{-1}')
grid
```

```
figure
for k=[0.0007, 0.007, 0.07]
[t, x] = f(k);
semilogy(t, x(:,2));
hold on;
end
xlabel('t (min)');
ylabel('B (cells/cm^{2})');
legend('k = 0.0007','k = 0.007','k = 0.07')
grid
```

Figure 39 Implementation of two ordinary differential equations 3.14 & 3.17 in MATLAB® using 4th order Runge-Kutta

The number of bacteria attached to the produce surface B (cells/cm^2) changing with time (min) is shown in Fig. 40, and number of bacteria suspended in water X (cells/ml) changing with time (min) is shown in Fig. 41. The initial concentration of bacteria carried into the domain by the flow was 10^6 cells/ml. As shown in Fig. 41, increasing the detachment rate constant k_{det}, number of bacteria suspended in water X increased at a given point in time. The bacteria suspended in water varied from 0 since the initial count of bacteria in water was zero at time t = 0, thus there was a rapid increase in the concentration of suspended bacteria in the tank due to the fluid flow coming into the reactor. Similarly, bacteria attached to the produce surface increased from 0. On the contrary, as shown in Fig. 40, the number of bacteria B attached to the surface decreased

when the k_{det} value increased. The two graphs represent the effect of detachment rate constant on cross-contamination behavior of bacteria. The results have shown that the detachment rate constant plays a vital role in mediation of bacteria detachment and attachment. k_{det} is mediated by shear force (Wang and Bryers, 1997), the equation for k_{det} is:

$$k_{det} = k_{det}^{0} \exp\left(\frac{\gamma F_b}{k_b T}\right)$$

.....(4.2)

where F_b is the bond force, and was calculated from total shear force F_t, given by the equation (4.3)

$$F_t = N_b A_c F_b$$

.....(4.3)

The results shown in the Fig. 40 & Fig. 41 have confirmed that shear force has important impact in mediating bacteria detachment. The cross-contamination can be controlled by modifying the velocity of fluid flow, and the extent of cross-contamination can be further predicted using the ODE model when no sanitizers/sanitizing agent is present.

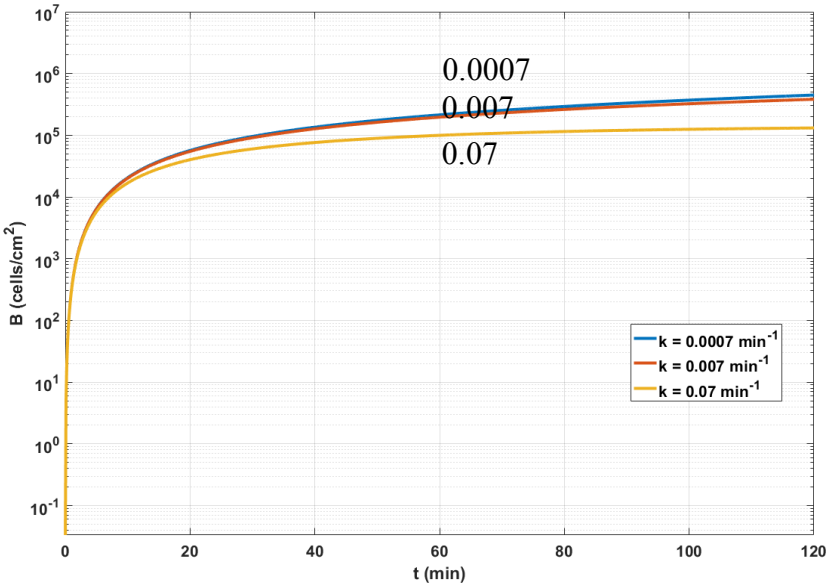

Figure 40 Change of bacteria suspended in water (B) as a function of time (t), as affected by k_{det}

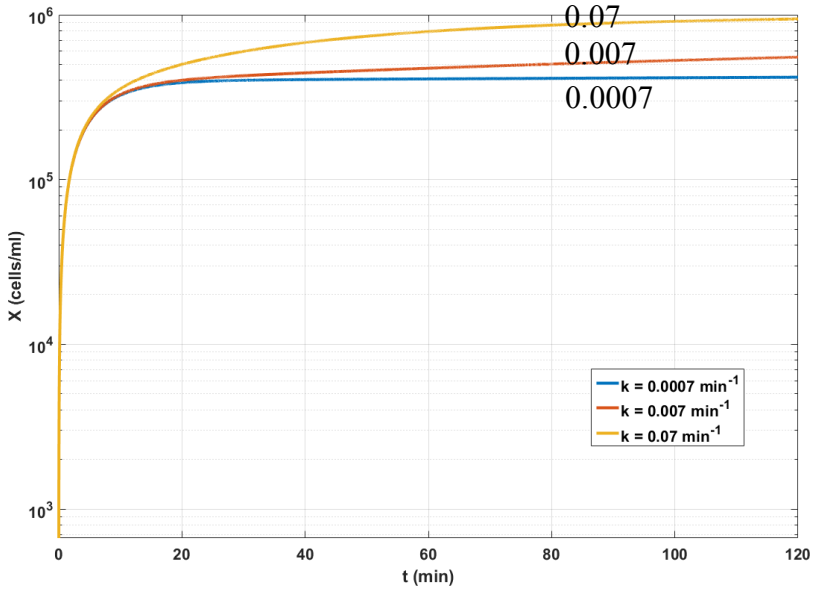

Figure 41 Change of bacteria removed/detached (X) as a function of time (t) as affected by k_{det}

4.5. ODE model results with sanitizers in water

In the previous section, sanitizers were not considered in the proposed equations. However, in practical commercial cases, physical treatments are coupled with chemical treatments to effectively inactivate and remove the bacteria attached on the produce, and inactivate the bacteria suspended in wash water to prohibit further cross contamination.

4.5.1. Prediction of bacterial detachment and attachment in the presence of sanitizers as a function of time

In section 2.4.1, the third equation (equation 3.18) for sanitizer was added. The number of bacteria suspended in water was a function of detachment rate constant and the chlorine concentration. In commercial processing environment, bacteria on fresh produce are removed by wash water as well as being inactivated by chemical sanitizers. To simulate cases in a real processing system, ODEs were developed to predict the transfer and inactivation of pathogens. The set of ordinary differential equations (equations 3.18, 3.19, 3.20, 3.21 discussed in section 3.4.1) was solved numerically by MATLAB®, codes as shown below in Fig 42.

$$\frac{dS}{dt} = D(S_{in} - S) - \lambda_c S - \beta_c OS \qquad (3.18)$$

$$\frac{dO}{dt} = k_0 \qquad (3.19)$$

$$\frac{dX}{dt} = D(X_{in} - X) - K_{adh} X \frac{A}{V} + k_{det} B \frac{A}{V} - \alpha XS \qquad (3.20)$$

$$\frac{dB}{dt} = K_{adh} X - k_{det} B \qquad (3.21)$$

The number of bacteria suspended in water (X (cells/ml)) is plotted as a function of time (min) in Fig. 43; the number of bacteria attached to the produce surface (B

(cells/cm^2)) is plotted as a function of time (min) in Fig. 44; chlorine concentration is plotted in Fig. 45 against time (min). The concentration of bacteria in the flowing flow was 10^6 cells/ml. Equations (3.18), (3.20) and (3.21) were solved numerically at three different initial chlorine concentrations: 20 mg/L, 0 mg/L and 200 mg/L. 20 mg/L was chosen because it is the commonly used dose in experimental scale washer. 0 mg/L and 200 mg/L are the extreme cases to study the effect of chlorine and the effect of detachment rate constant in the absence/presence of a sanitizer.

```
function [] = sanitizer2(init_val)
% define the system of three ode equations
% define x(1), x(2), x(3)
% define the detachment constant k, k = 0.007,0.07,0.7 (changes by 10 times)
% the unit for S is ppm

% Initial concentration of X (bacteria left in water) is 6log;
% Dose of chlorine added is 20ppm;

% syms t x k
f = @(t,x,k)[2/30*((10^6)-x(1))-0.01*10*x(1)+10*k*x(2)-0.75*x(1)*x(3); 0.01*x(1)-k*x(2); 2/30*(init_val-
x(3))-0.0017*x(3)-0.000538*(32.3*t)*x(3)];


figure(1)
for k = [0.007, 0.07, 0.7]
    [t,xk] = ode45 (@(t,x) f(t,x,k),[0:0.01:60],[0 0 0]);
    semilogy(t,xk(:,1));
    hold on;
end
xlabel('t (min)');
ylabel('X (cells/ml)');
legend('k=0.007 min^{-1}', 'k=0.07 min^{-1}', 'k=0.7 min^{-1}')
grid

figure(2)
for k = [0.007, 0.07, 0.7]
    [t,xk] = ode45 (@(t,x) f(t,x,k),[0:0.01:60],[0 0 0]);
    semilogy(t,xk(:,2));
    hold on;
end
xlabel('t (min)');
ylabel('B (cells/cm^2)');
legend('k=0.007 min^{-1}', 'k=0.07 min^{-1}', 'k=0.7 min^{-1}')
grid

figure(3)
for k = [0.007, 0.07, 0.7]
    [t,xk] = ode45 (@(t,x) f(t,x,k),[0:0.01:60],[0 0 0]);
    plot(t,xk(:,3));
    hold on;
end
xlabel('t (min)');
ylabel('S (ppm)');
% legend('k=0.007', 'k=0.07', 'k=0.7')
grid
end
```

Figure 42 Implementation of ODEs for variables B (bacteria attached to the produce surface), X (bacteria suspended in water) and S (concentration of sanitizer in water) in MATLAB® using ODE solver ode45

At chlorine concentration S_{in} = 20 mg/L

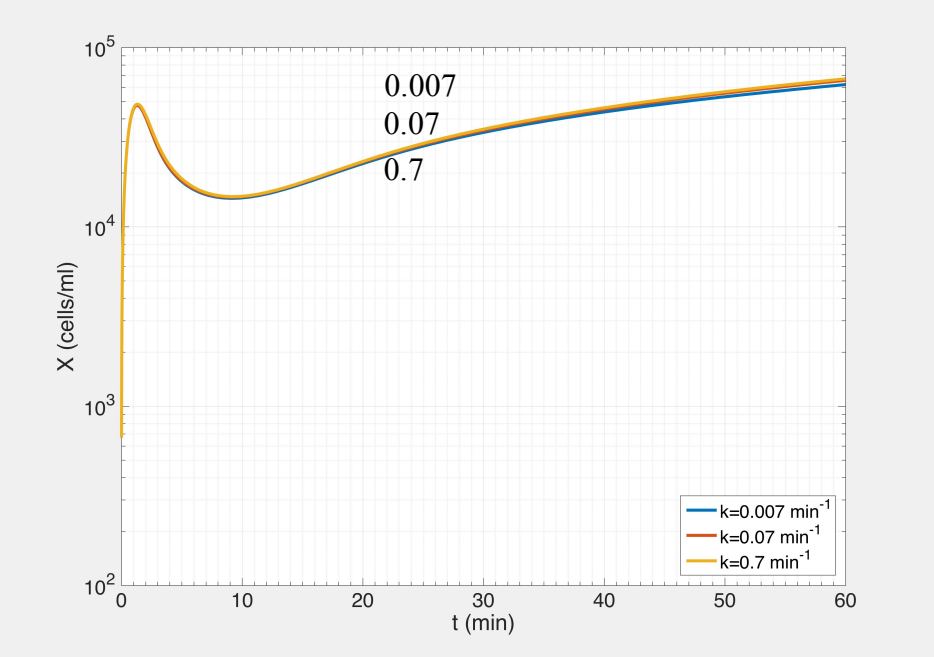

Figure 43 Suspended bacteria in water as a function of time at different k_{det}, in the presence of a sanitizer (S_{in} = 20 mg/L)

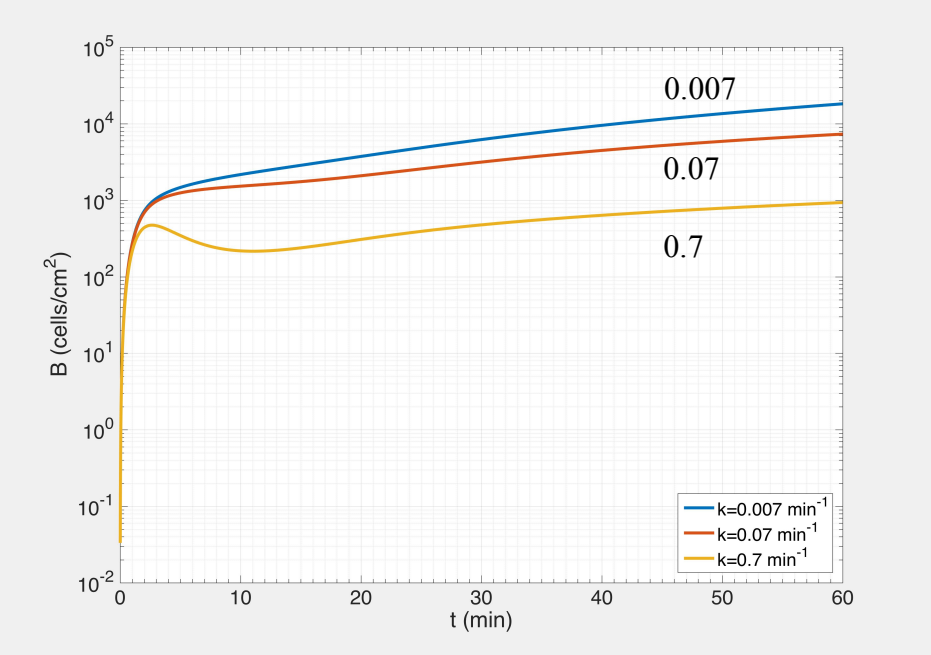

Figure 44 Bacteria attached to the surface as a function of time at different k_{det}, in the presence of a sanitizer (S_{in} = 20 mg/L)

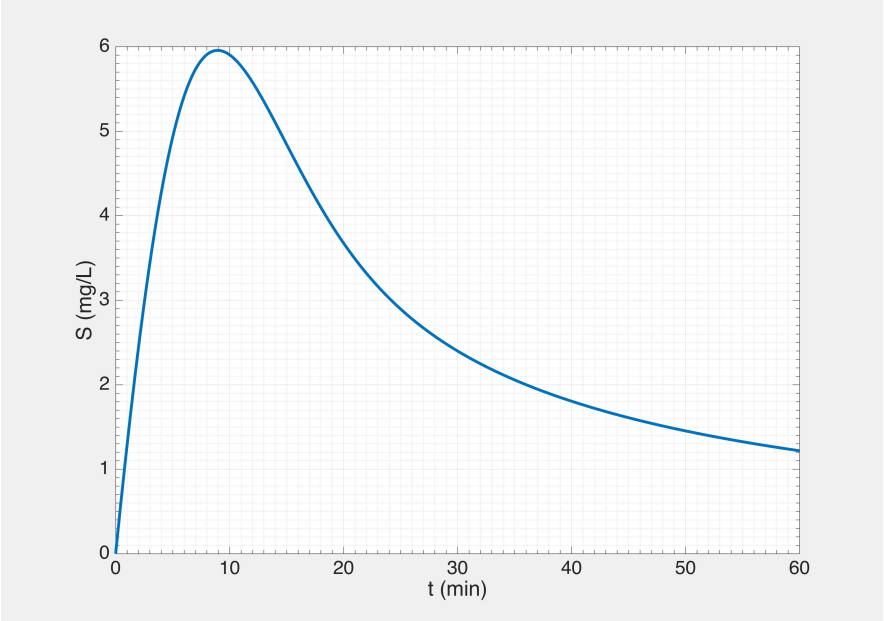

Figure 45 Change of chlorine concentration with time at initial chlorine concentration (S_{in} = 20 mg/L)

Fig. 43, Fig. 44, and Fig. 45 show the change of X (bacteria suspended in water), B (bacteria attached) and S (chlorine concentration) as a function of time, when the initial chlorine concentration is 20 mg/L. In Fig. 43, during the washing process (60 min), the number of X increased from 0 (no bacteria within the tank) at t = 0, and greatly increased in the very initial stage when fluid flow containing bacteria load of 10^6 starts entering the washer tank. Meanwhile, in Fig. 44, there is a steep increase in chlorine concentration in the first 10 min, which is due to the continuous replenishment of chlorine. While bacteria enter the washer tank, chlorine was largely consumed by bacteria, thus there's a decrease of chlorine concentration. From t = 10 min, the number of bacteria in water (X) slowly increases, whereas the concentration of chlorine decreases. It can be resulted from the natural decay of chlorine, the depletion of chlorine by chemical oxygen demand and consumptions due to organic substances (in pilot plant scale equipment, as well as in the

commercial processing system, there were multiple types of organic (and inorganic) materials in wash water, i.e., the bacteria, plant juices, soil debris (Munther et al., 2015)).

In Fig. 44, when increasing detachment rate constant k_{det}, no increase was seen on the number of bacteria suspended (X); however, in Fig. 45, when k_{det} increased, the number of bacteria significantly decreased. It demonstrated that the bacteria attached to the surface may be greatly affected by detachment rate constant, but not by the concentration of chlorine. To further study the effect of chlorine and k_{det} on X and B, extreme cases when chlorine concentration is 0 mg/L and 200 mg/L were studied. The results are shown in Figs. 46 -50.

At chlorine concentration S_{in} = 0 mg/L

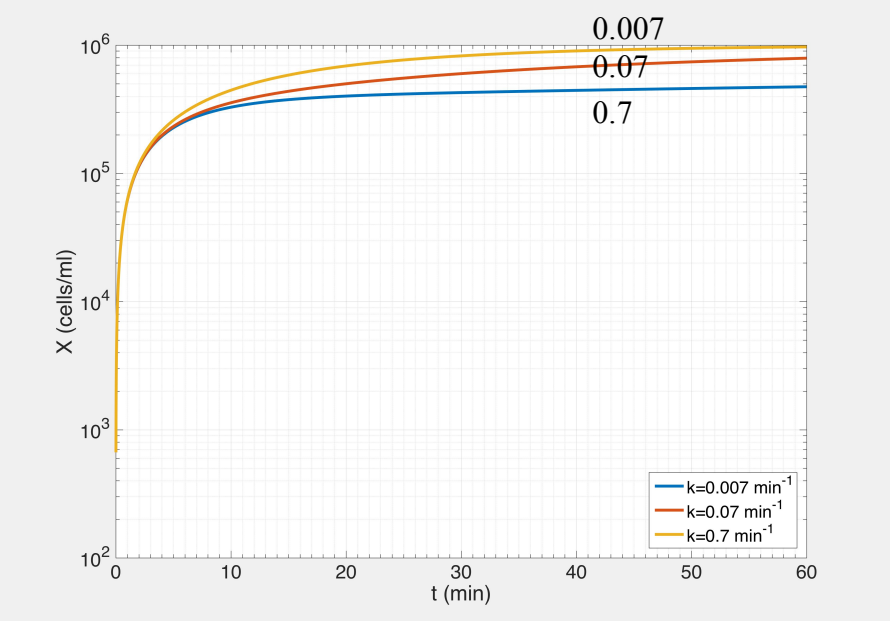

Figure 46 Bacteria suspended in water as a function of time at different k_{det}, in the absence of a sanitizer (S_{in} = 0 mg/L)

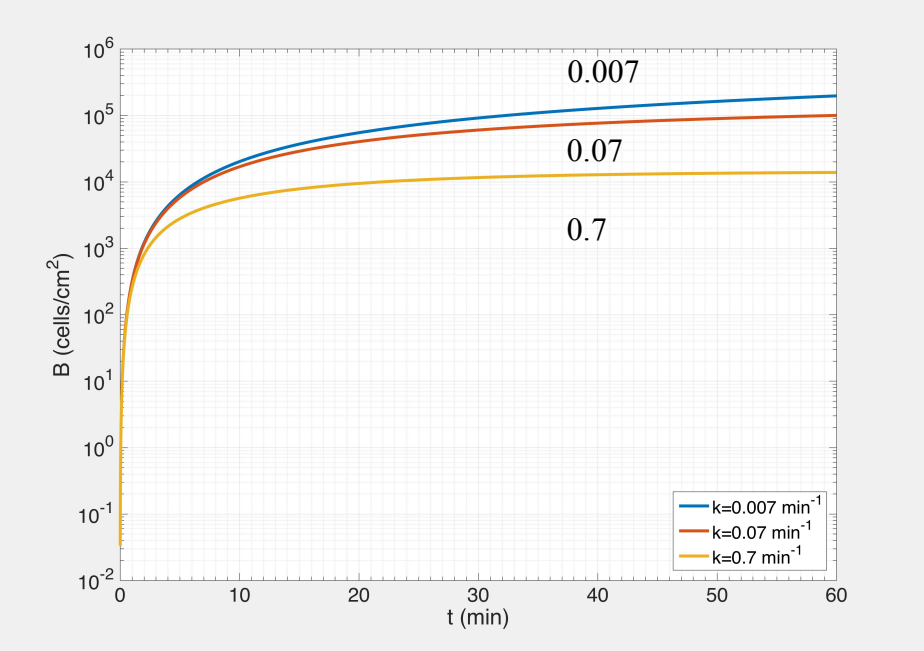

Figure 47 Bacteria attached to the surface as a function of time at different k_{det}, in the absence of a sanitizer (S_{in} = 0 mg/L)

In Fig. 46 and Fig. 47 when there was no sanitizer in water, when k_{det} increased, the bacteria suspended in water increased; but the bacteria attached to surface decreased. It can be seen that detachment rate constant plays an important role in mediating bacteria detachment and attachment when only physical shear forces applied.

At chlorine concentration S_{in} = 200 mg/L

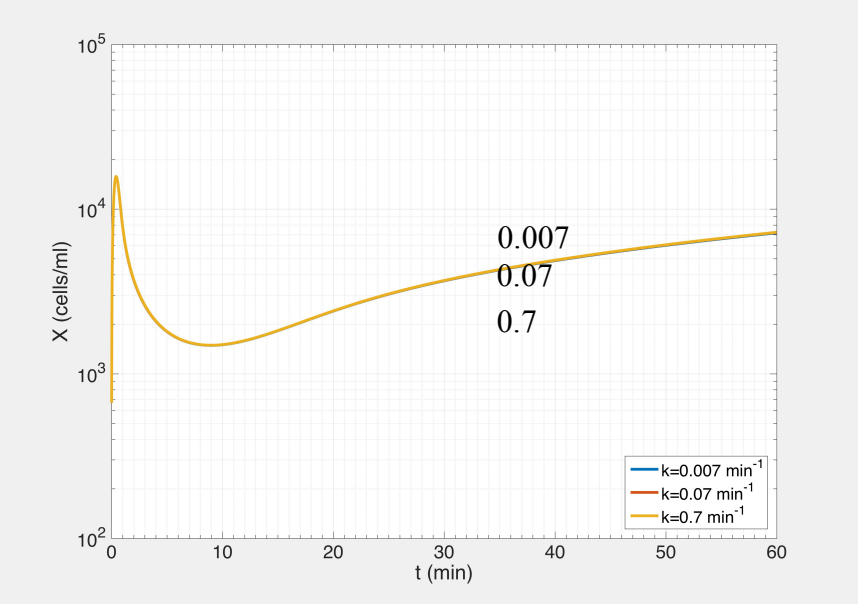

Figure 48 Bacteria suspended in water as a function of time at different k_{det}, in the presence of a sanitizer (S_{in} = 200 mg/L)

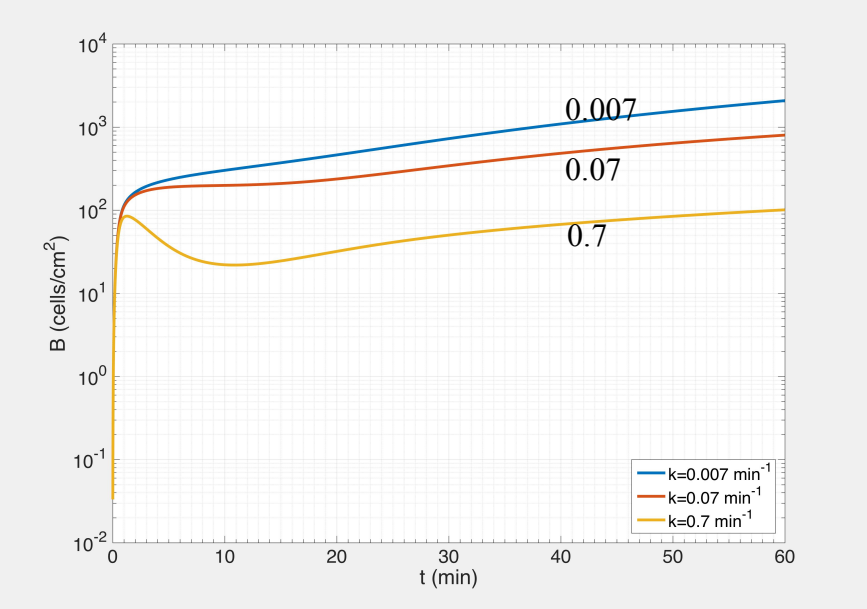

Figure 49 Bacteria attached to the surface as a function of time at different k_{det}, in the presence of a sanitizer (S_{in} = 200 mg/L)

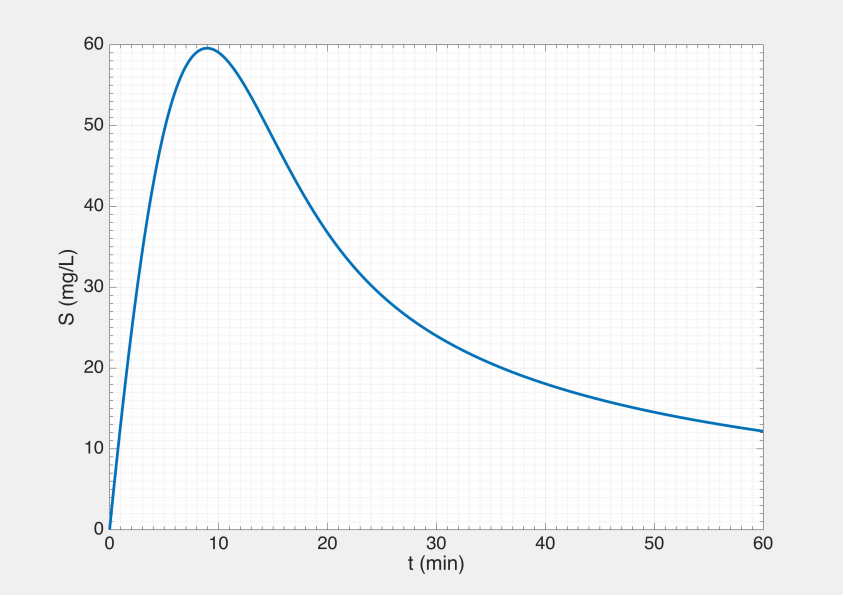

Figure 50 Change of chlorine concentration by time at initial chlorine concentration (S_{in} = 200 mg/L)

In Fig. 48, no change in the variation of X was seen when k_{det} increased. The bacteria suspended were inactivated by sanitizer and the amount of X decreased quickly. Unlike the change of X in Fig. 43, the bacteria suspended were mostly inactivated by chlorine even when the chlorine concentration decreased, as shown in Fig. 50. Fig. 49 shows the change of bacteria attached to the surface. It can be seen that at S_{in} = 200 mg/L, when k_{det} increased, there was still a decrease in B. The effect of detachment rate constant shows a more dominant effect on the bacteria attached, than the chlorine concentration. This is in agreement with our assumption that the free chlorine inactivated the free bacteria left in water, but not the bacteria attached on the surface, the bacteria attached on the surface was removed by mechanical force. Therefore, chemical treatment can be coupled with the physical treatment to enhance the sanitation process for the inactivation and removal of bacteria. The bacteria on the deposition surface could be removed by shear force and thus

detached from the surface, the bacteria suspended in water were further inactivated by chlorine. The whole process can be regarded as an indirect inactivation by chlorine.

5. CONCLUSIONS

COMSOL® Multiphysics was used to numerically simulate the flow field and to calculate shear stress values in an experimental benchtop washing device, to understand the effect of shear stress on (a) the detachment of bacteria from produce surface to wash water and (b) the attachment of bacteria to produce surface from wash water containing contaminated organic load.

Numerical results from the detachment studies indicated that the average shear stress exerted on the leaf surface was between 28 mPa and 109 mPa, when the disk rotating speed was varied between 100 rev/min to 200 rev/min. The experimental results (done by Dr. Nitin's group at UC Davis) showed that the corresponding detachment of *E. coli* O157:H7-*lux* varied between 1 log CFU/cm^2 and 1.5 log CFU/cm^2. For the attachment study, bacteria inoculated particles were suspended in water to study the transfer and the attachment of bacteria from the particles to leaf surface under shear. In the presence of suspended particles (diameter 100 μm), the shear stress varied between 137 mPa and 403 mPa. Experimental data showed some (up to 0.4%) bacteria were transferred to the leaf surface suggesting that transfer and attachment can take place in the presence of shear stress.

The point-attachment model using ordinary differential equations to describe the ligand-receptor binding of bacteria and produce surface was used to quantify the detachment and attachment of bacteria as a function of time. Literature has shown that the detachment of bacteria is related to the detachment rate constant and the rate constant is a function of shear stress. Experimental (at UC Davis) and numerical results have shown that the shear stress exerted on produce surface can enhance the removal of

bacteria from the plant surface during washing. Organic particles can increase the shear stress induced by fluid flow while bacterial attachment can still take place in presence of shear stress. Preliminary results have shown that detachment rate constant depends on the shear and preliminary MATLAB® results have reflected that the detachment rate constant is effective in bacterial detachment and attachment.

Improved ordinary differential equations were developed where the efficacy of sanitizers was considered mathematically. In the presence of a sanitizer, the inactivation of bacteria was dominantly controlled by the sanitizer, instead of detachment rate constant. However, detachment rate constant still played a vital role in the removal of bacteria in the whole process.

The numerical study of detachment and attachment of bacteria has given some insights into the mechanism of cross-contamination and provided a strategy in controlling the behavior by mediating the fluid flow. The mathematical equations can be a useful tool in the prediction of cross-contamination during produce washing. Also, it could be helpful in modifying parameters in washing system to enhance the safety of fresh produce.

6. FUTURE WORK

Further work can focus on the following aspects:

1. The roughness of biological surface can be considered in the numerical simulation. Roughness can shelter the microbes.
2. In the experiments, lettuce leaves were cut in circular shapes and the surface was relatively smooth. The effect of chlorine on the bacteria inhabited in the grooves or valleys on the surface should be investigated.
3. Experiments should be conducted to quantitatively study the correlation between k_{det} and shear stress, so as to optimize the mathematical model.
4. Shear stress results from COMSOL® should be coupled with MATLAB® results to quantify cross-contamination under shear.
5. The flow in washer containing multiple produce can be simulated numerically. The interaction of produce to produce and the bacteria transfer among produce could be quantified and numerically simulated.

7. REFERENCES

1. An, Y. H., & Friedman, R. J. (1997). Laboratory methods for studies of bacterial adhesion. Journal of Microbiological Methods, 30(2), 141-152.
2. Artés, F., Gómez, P., Aguayo, E., Escalona, V., & Artés-Hernández, F. (2009). Sustainable sanitation techniques for keeping quality and safety of fresh-cut plant commodities. Postharvest Biology and Technology, 51(3), 287-296.
3. Aubert, M. C., Elluard, M. P., & Barnier, H. (1993). Shear stress induced erosion of filtration cake studied by a flat rotating disk method. Determination of the critical shear stress of erosion. Journal of membrane science, 84(3), 229-240.
4. Bos, R., Van der Mei, H. C., & Busscher, H. J. (1999). Physico-chemistry of initial microbial adhesive interactions–its mechanisms and methods for study. FEMS microbiology reviews, 23(2), 179-230.
5. Brown, D. C., & Larson, R. S. (2001). Improvements to parallel plate flow chambers to reduce reagent and cellular requirements. BMC immunology, 2(1), 9.
6. Busscher, H. J., & van der Mei, H. C. (2012). How do bacteria know they are on a surface and regulate their response to an adhering state?. PLoS pathogens, 8(1), e1002440.
7. Busscher, H. J., Doornbusch, G. I., & Van der Mei, H. C. (1992). Adhesion of mutans streptococci to glass with and without a salivary coating as studied in a parallel-plate flow chamber. Journal of dental research, 71(3), 491-500.
8. Cozens-Roberts, C., Lauffenburger, D. A., & Quinn, J. A. (1990). Receptor-mediated cell attachment and detachment kinetics. I. Probabilistic model and analysis. Biophysical journal, 58(4), 841-856.
9. D.C. Wilcox, Turbulence Modeling for CFD, 2nd ed., DCW Industries, 1998
10. De Giusti, M., Aurigemma, C., Marinelli, L., Tufi, D., De Medici, D., Di Pasquale, S., De Vito, C., & Boccia, A. (2010). The evaluation of the microbial safety of fresh ready-to-eat vegetables produced by different technologies in Italy. Journal of applied microbiology, 109(3), 996-1006.

11. De Jong, P., Te Giffel, M. C., & Kiezebrink, E. A. (2002). Prediction of the adherence, growth and release of microorganisms in production chains. International journal of food microbiology, 74(1-2), 13-25.
12. De La Fuente, L., Montanes, E., Meng, Y., Li, Y., Burr, T. J., Hoch, H. C., & Wu, M. (2007). Assessing adhesion forces of type I and type IV pili of Xylella fastidiosa bacteria by use of a microfluidic flow chamber. Applied and environmental microbiology, 73(8), 2690-2696.
13. Dickinson, R. B., & Cooper, S. L. (1995). Analysis of shear-dependent bacterial adhesion kinetics to biomaterial surfaces. AIChE Journal, 41(9), 2160-2174.
14. Evans, E. A. (1985). Detailed mechanics of membrane-membrane adhesion and separation. II. Discrete kinetically trapped molecular cross-bridges. Biophysical journal, 48(1), 185-192.
15. Evans, E. A. (1985). Detailed mechanics of membrane-membrane adhesion and separation. I. Continuum of molecular cross-bridges. Biophysical journal, 48(1), 175-183.
16. Faille, C., Dennin, L., Bellon-Fontaine, M. N., & Benezech, T. (1999). Cleanability of stainless steel surfaces soiled by Bacillus thuringiensis spores under various flow conditions. Biofouling, 14(2), 143-151.
17. FDA. (2015). Raw produce: Selecting and serving it safely. , http://www.fda.gov/Food/ResourcesForYou/Consumers/ucm114299.htm.
18. Fink, R., Oder, M., Rangus, D., Raspor, P., & Bohinc, K. (2015). Microbial adhesion capacity. Influence of shear and temperature stress. International journal of environmental health research, 25(6), 656-669.
19. Gil, M. I., Selma, M. V., López-Gálvez, F., & Allende, A. (2009). Fresh-cut product sanitation and wash water disinfection: problems and solutions. International journal of food microbiology, 134(1-2), 37-45.
20. Hammer, D. A. & Lauffenburger, D. A. (1987). A dynamical model for receptor-mediated cell adhesion to surfaces. Biophysical journal, 52(3), 475-487.
21. Hammer, D. A., & Lauffenburger, D. A. (1989). A dynamical model for receptor-mediated cell adhesion to surfaces in viscous shear flow. Cell biophysics, 14(2), 139-173.

22. Heilmann, C., Schweitzer, O., Gerke, C., Vanittanakom, N., Mack, D., & Götz, F. (1996). Molecular basis of intercellular adhesion in the biofilm-forming Staphylococcus epidermidis. Molecular microbiology, 20(5), 1083-1091.
23. Hermansson, M. (1999). The DLVO theory in microbial adhesion. Colloids and Surfaces B: Biointerfaces, 14(1-4), 105-119.
24. James, M. L., Smith, G. M., & Wolford, J. C. (1985). Applied numerical methods for digital computation (Vol. 2). New York: Harper & Row.
25. Jensen, D. A., Friedrich, L. M., Harris, L. J., Danyluk, M. D., & Schaffner, D. W. (2015). Cross contamination of Escherichia coli O157: H7 between lettuce and wash water during home-scale washing. Food microbiology, 46, 428-433.
26. Katsikogianni, M., & Missirlis, Y. F. (2004). Concise review of mechanisms of bacterial adhesion to biomaterials and of techniques used in estimating bacteria-material interactions. Eur Cell Mater, 8(3), 37-57.
27. Lelièvre, C., Antonini, G., Faille, C., & Bénézech, T. (2002). Cleaning-in-Place: modelling of cleaning kinetics of pipes soiled by Bacillus spores assuming a process combining removal and deposition. Food and Bioproducts Processing, 80(4), 305-311.
28. LELIEVRE, C., FAILLE, C., & BENEZECH, T. (2001). Removal kinetics of Bacillus cereus spores from stainless steel pipes under CIP procedure: influence of soiling and cleaning conditions. Journal of food process engineering, 24(6), 359-379.
29. Levich, Veniamin G., and Raymond J. Seeger. (1963). Physicochemical hydrodynamics. American Journal of Physics 31(11), 892-892.
30. Lopez-Galvez, F., Gil, M. I., Truchado, P., Selma, M. V., & Allende, A. (2010). Cross-contamination of fresh-cut lettuce after a short-term exposure during pre-washing cannot be controlled after subsequent washing with chlorine dioxide or sodium hypochlorite. Food Microbiology, 27(2), 199-204.
31. Luo, Y., Nou, X., Millner, P., Zhou, B., Shen, C., Yang, Y., ... & Shelton, D. (2012). A pilot plant scale evaluation of a new process aid for enhancing chlorine efficacy against pathogen survival and cross-contamination during produce wash. International Journal of Food Microbiology, 158(2), 133-139.
32. Luo Y., Nou X., Yang Y., Alegre I., Turner E., Feng H., Abadias M., & Conway W. (2011). Determination of Free Chlorine Concentrations Needed To Prevent

Escherichia coli O157:H7 Cross-Contamination during Fresh-Cut Produce Wash. Journal of food protection, 74(3), 352-358.

33. Morra, M. & Cassinelli, C. (1998). Bacterial adhesion to polymer surfaces: a critical review of surface thermodynamic approaches. Journal of Biomaterials Science, Polymer Edition, 9(1), 55-74.
34. Rodgers, S. L., Cash, J. N., Siddiq, M., & Ryser, E. T. (2004). A comparison of different chemical sanitizers for inactivating Escherichia coli O157: H7 and Listeria monocytogenes in solution and on apples, lettuce, strawberries, and cantaloupe. Journal of food protection, 67(4), 721-731.
35. Schlichting, H., Gersten, K., Krause, E., Oertel, H., & Mayes, K. (1979). Boundary-layer theory (Vol. 7). New York: McGraw-hill.
36. Schmid-Schoenbein, G. W., Fung, Y. C., & Zweifach, B. W. (1975). Vascular endothelium-leukocyte interaction; sticking shear force in venules. Circulation research, 36(1), 173-184.
37. Sharma, R. R., Demirci, A., Puri, V. M., Beuchat, L. R., & Fett, W. F. (2004). Modeling the inactivation of Escherichia coli O157: H7 on inoculated alfalfa seeds during exposure to ozonated or electrolyzed oxidizing water. Transactions of the ASAE, 47(1), 173.
38. Shaw, R. K., Berger, C. N., Feys, B., Knutton, S., Pallen, M. J., & Frankel, G. (2008). Enterohemorrhagic Escherichia coli exploits EspA filaments for attachment to salad leaves. Applied and Environmental Microbiology, 74(9), 2908-2914.
39. Sirinutsomboon, B., & Delwiche, M. J. (2013). Effect of fluid flow on attachment of Escherichia coli O137: H41 to plant surface structure analogs built by microfabrication. Biological Engineering Transactions, 6(2), 83-104.
40. Vaudaux, P., Yasuda, H., Velazco, M. I., Huggler, E., Ratti, I., Waldvogel, F. A., ... & Proctor, R. A. (1990). Role of host and bacterial factors in modulating staphylococcal adhesion to implanted polymer surfaces. Journal of biomaterials applications, 5(2), 134-153.
41. Vuong, C. & Otto, M. (2002). Staphylococcus epidermidis infections. Microbes and infection, 4(4), 481-489.

42. Wang, G. T. Y., & Bryers, J. D. (1997). A dynamic model for receptor-mediated specific adhesion of bacteria under uniform shear flow. Biofouling, 11(3), 227-252.
43. Wang, H., Liang, W., Feng, H., & Luo, Y. (2007). Modeling of the effect of washing solution flow conditions on Escherichia coli O157: H7 population reduction on fruit surfaces. Journal of food protection, 70(11), 2533-2540.
44. Warning, A. & Datta, A. K. (2013). Interdisciplinary engineering approaches to study how pathogenic bacteria interact with fresh produce. Journal of Food Engineering, 114(4), 426-448.